Proceedings of the Geologists' Association 135 (2024) 61–77

Contents lists available at ScienceDirect

Proceedings of the Geologists' Association

journal homepage: www.elsevier.com/locate/pgeola

The influence of bedrock faulting and fracturing on sediment availability and Quaternary slope systems, Talla, Southern Uplands, Scotland, UK

Katie Whitbread *, Chris Thomas, Andrew Finlayson

British Geological Survey, The Lyell Centre, Research Avenue South, Edinburgh EH14 4AP, UK

ARTICLE INFO

Article history:
Received 16 March 2023
Received in revised form 15 November 2023
Accepted 16 November 2023
Available online 9 December 2023

Keywords:
Hillslope processes
Bedrock faulting
Sediment connectivity
Connectivity index
Upland landscapes
Quaternary
Slopes

ABSTRACT

In bedrock-dominated upland terrains, local heterogeneity in the erodibility of rock masses is a critical but under-explored factor constraining sediment erosion, mobilisation and transport. Here we examine how fault-related fracturing controls variations in the erodibility and grain-size of bedrock source material at the hillslope-scale. We then assess how this influences the evolution of slope sediment systems using a case-study from the Southern Uplands, Scotland, UK. Faults are associated with fracture densities that are an order of magnitude greater than background joint- and bedding-related fractures in weakly metamorphosed sedimentary rocks. Thus, fault zones are enhanced source areas yielding more abundant, smaller clasts. They are associated with enhanced erosion, gullying and debris flows, and the development of blanket colluvium on steep open hillsides. The orientation at which faults intersect the hillslope constrains the evolution of the sediment system. Faults with trends closely aligned to the direction of slope are associated with higher erosion *via* confined-channel debris flow activity in strongly coupled gullies. Faults that are oblique to slope direction disrupt and segment gully systems developed on minor transfer faults. Overall, faults that are oblique to slope direction are associated with lower erosion and give rise to decoupling within debris flow systems. Inclusion of geological weighting parameters in the formulation of a sediment connectivity index to characterise the effect of faulting on the erodibility and mobility of source material improves correspondence of the model with observations and provides a simple approach that could be adapted for other sources of geological heterogeneity.

1. Introduction

Erosion, mobilisation and transport of sediment from slopes to channels are important landscape responses to climatic, tectonic and anthropogenic perturbation. In upland settings, slope stability and sediment processes are key controls on long-term landscape change (*e.g.,* Willgoose et al., 1991; Burbank et al., 1996; Wolf et al., 2022), but can also present a range of hazards and practical management challenges for transport, energy and water infrastructure, especially under changing climate regimes (*e.g.,* Haeberli et al., 2017; Finlayson, 2020; Palamakumbura et al., 2021). The nature of these slope processes is strongly conditioned by the availability of material for erosion and transport. On many upland slopes bedrock is commonly found at or near the surface (particularly areas unaffected by, or with limited cover of, glacial deposits) and therefore sediment availability is determined by spatial patterns of weathering and erosion affecting *in situ* rock (*e.g.,* Neely et al., 2019; Palamakumbura et al., 2021). Heterogeneity in rock mass strength has long been recognised as a major control on slope stability (*e.g.,* Hoek, 1999; Hoek and Brown, 2019), and recent work has highlighted its conditioning role in slope sediment processes (Molnar et al., 2007; Roy et al., 2016; DiBiase et al., 2018; Neely and DiBiase, 2020). In particular, fractures within the rock mass have been identified as a major control on the availability and grain-size distribution of source material for rockfall (Wang et al., 2020), colluvial and debris flow processes (Sklar et al., 2017; Neely and DiBiase, 2020), and fluvial erosion (Scott and Wohl, 2018).

At the landscape-scale, differences in fracture density, and the consequent influence on sediment grain-size, constrain the relief of mountain ranges by influencing the slope of rock cliffs and riverbeds (Shobe et al., 2016; DiBiase et al., 2018; Neely and DiBiase, 2020). However, variations in fracture density can be highly localised. For example, fault-related deformation commonly occurs in linear 'damage zones' tens of metres wide flanking a fault plane (*e.g.,* Faulkner et al., 2010; Mitchell and Faulkner, 2012; Choi et al., 2016; Wang et al., 2021). Such local-scale effects may influence slope stability, sediment erosion and transport processes at the scale of sub-catchments and individual slopes (*e.g.,* Roy et al., 2016), and potentially have significant implications for hazard susceptibility, environmental management and infrastructure design.

This study assesses how strong local variations in fracture density, caused by faulting, control slope erosion and transport processes within

* Corresponding author.
E-mail address: kwhi@bgs.ac.uk (K. Whitbread).

https://doi.org/10.1016/j.pgeola.2023.11.003

a post-glacial upland landscape in the Southern Uplands of Scotland, UK. The study area in the Tweedsmuir Hills has been selected to compare the impact of differences in the angle at which faults intersect a slope on the development of a post-glacial sediment system. Geomorphic mapping (*e.g.*, Finlayson, 2020), coupling relationships (*e.g.*, Fryirs et al., 2007), and slope–channel connectivity analysis (*cf.*, Borselli et al., 2008; Cavalli et al., 2013) are used to characterise slope systems at scales relevant for informing conceptual ground models (*e.g.*, Norbury, 2021) and hazard assessment (*e.g.*, Wang et al., 2020).

2. Geological setting

The Tweedsmuir Hills are located near the centre of Scotland's Southern Uplands (Fig. 1). The study site lies at the head of the Talla Reservoir and includes the lower reaches of the Games Hope Burn and the Talla Water, as well as the minor catchment of the Codleteth Burn north of Talla Linnfoots. Talla Reservoir was constructed between 1897 and 1904 to supply water to the city of Edinburgh. It lies within an upland landscape ranging in elevation from the reservoir level at approximately 290 m above Ordnance Datum (aOD) to an undulating upland plateau over 600 m aOD with local summits at approximately 730 m aOD. The primary land use is rough grazing, although replanting of woodland is ongoing in much of the upper Gameshope catchment.

The Southern Uplands terrane is underlain by deformed and metamorphosed turbiditic sandstone, with interbedded siltstone and mudstone of Ordovician to Silurian age. The succession forms a compressed accretionary complex consisting of a series of stacked thrust sheets formed during continental collision between Laurentia and Avalonia. These thrust-bound sheets have been rotated towards the vertical during the latter phases of the collision, forming northeast- to southwest-striking structural tracts bound by subvertical reverse faults (Stone, 2014). Bedding within the structural tracts strikes roughly northeast–southwest, sub-parallel to the tract boundaries,

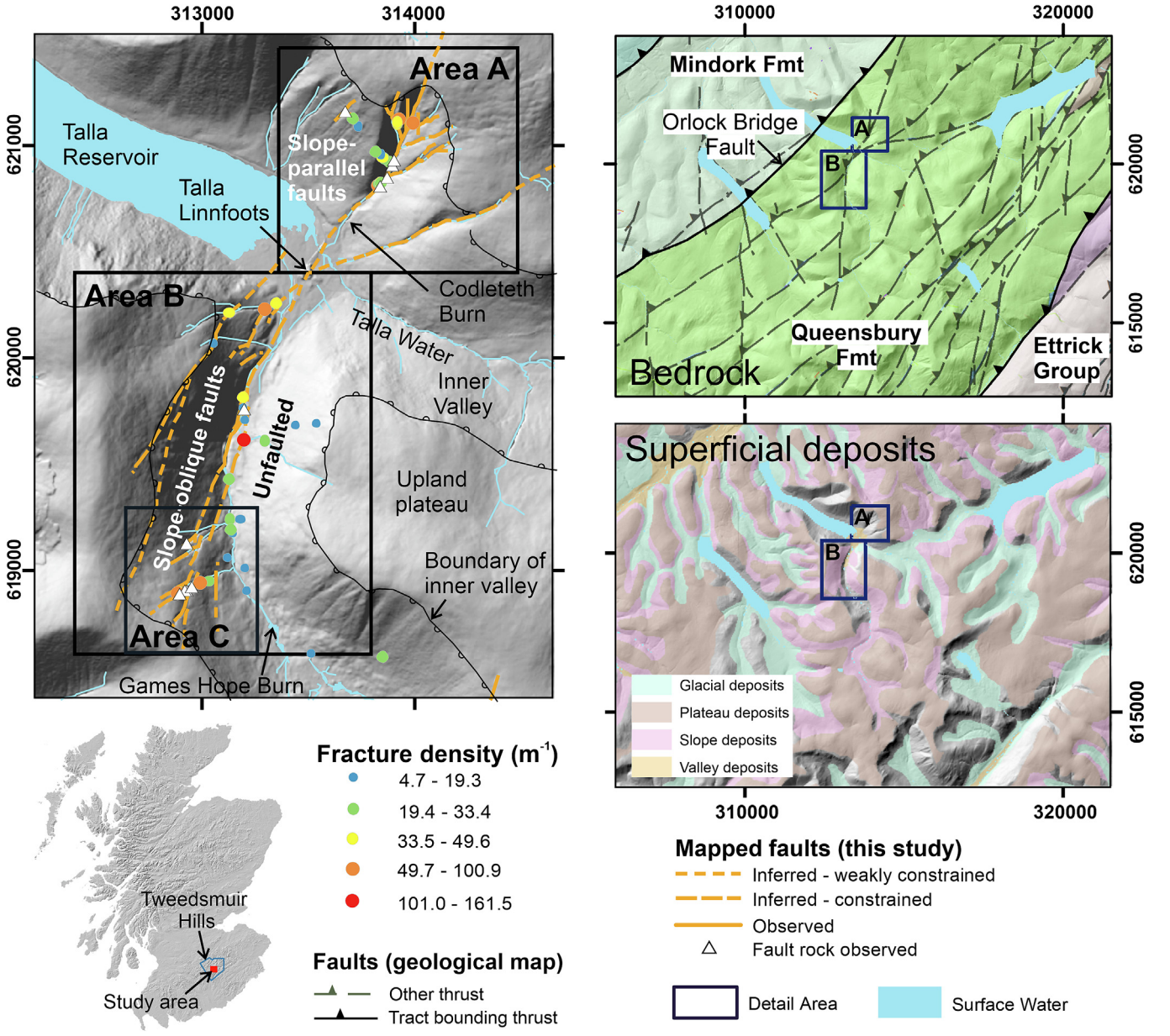

Fig. 1. Topography of the study area showing the location of mapped faults, observed fault gouge and fracture density measurements (left hand map). Areas A–C refer to study locations discussed in the text (A — Codleteth Burn, B — Gameshope, C — Gameshope gullies).

and is steeply dipping to vertical, and in places overturned (British Geological Survey, 2009).

Numerous strike-parallel minor thrusts occur within the fault-bound tracts. These reverse faults are locally displaced by sets of cross-strike structures orientated north–northeast to south–southwest and northwest to southeast (Fig. 1). The former commonly display sinistral displacement, with dextral displacement more commonly associated with the latter. Both the thrusts and cross-strike faults are likely to have been reactivated during regional deformation associated with the later stages of the Caledonian orogeny and due to far-field effects associated with the Variscan and Alpine orogenies (Stone et al., 2012).

The cross-strike faults are typically associated with brittle fracture, with narrow zones of fault gouge noted, and are thought to have been active since a phase of granite intrusion that occurred in the final stage of the continental collision in the early Devonian (*c.*, 400 Ma) (Stone et al., 2012). These bands of fractured rock contrast with surrounding unfaulted bedrock, in which discontinuities are related to bedding structures and joints formed during rock burial under regional tectonic stresses (Stone et al., 2012).

The study area is in the thrust tract associated with the Gala Group (Llandovery), which is bound to the north by the Orlock Bridge Fault, and to the south by a faulted boundary with the Ettrick Group (Fig. 1). The underlying bedrock comprises wacke-type sandstone of the Queensberry Formation. The sandstone is typically medium to very coarse-grained, with beds 0.3 to 3 m thick. It is interbedded in places with siltstone-dominated bands up to 20 m thick comprising beds of siltstone 0.2 to 1 m thick and 1–5 m thick beds of conglomerate (British Geological Survey, 2009).

The Southern Uplands have been shaped by erosion during repeated phases of crustal exhumation throughout the Mesozoic and Cenozoic associated with rifting and the emplacement of the British and Irish Paleogene Igneous Province (*e.g.,* Holford et al., 2010; Hudson, 2011; Łuszczak et al., 2014; Cogné et al., 2016; Fame et al., 2018). The resulting landscape, comprising a rolling plateau dissected by broad, smooth-sided fluvial valleys, generally displays relatively limited evidence of glacial modification despite repeated Quaternary glaciations (Ballantyne, 2021). However, evidence for localised glacial erosion is found in the region of the Tweedsmuir Hills, which comprise the highest part of the Southern Uplands terrane. In this area, zones of selective linear erosion have given rise to glacial troughs ("inner valleys") and cirques cut into the undulating plateau (Fig. 1; Pearce et al., 2014; Sugden, 1968).

The Tweedsmuir Hills formed an ice centre during the latter phases of the Late Devensian glaciation and briefly hosted a small plateau ice cap which fed valley glaciers during the Younger Dryas (12.9–11.7 ka) (Pearce et al., 2014; Ballantyne, 2021). Glacial deposits are restricted to valley bottoms and lower slopes and include areas of till and terminal, lateral and hummocky moraines developed locally as small ridges and mounds on valley floors. In the study area, small morainic mounds occur locally in the lower Gameshope catchment, and a well-developed outwash fan system occurs just to the north, where the Gameshope and Talla catchments merge at Talla Linnfoots (Pearce et al., 2014).

An extensive mantle of regolith formed by frost-weathering of bedrock is present on plateau areas (Ragg and Bibby, 1966; Ballantyne, 2021). The regolith is likely to have been formed under periglacial conditions prior to the Late Devensian glaciation, indicating that the ice-cover over higher ground was cold-based and associated with limited erosion (Ragg and Bibby, 1966; Ballantyne, 2021). The regolith is the main source material for solifluction lobes, which have formed locally on the upland plateau (here mapped as 'Head' deposits), and colluvial deposits which are present on some inner valley slopes. The latter are indicated by terracettes formed by surface wash and down-slope creep of the loose, fractured rock and associated soil (Ragg and Bibby, 1966).

Previous geological and geomorphic mapping indicates that bedrock occurs at or near surface throughout much of the inner, glacially scoured valleys. Thin till is locally present on valley side walls, and moraines, other glacial deposits and alluvium are restricted to the valley floors (British Geological Survey, 1987; Pearce et al., 2014). Scree and frost-shattered bedrock occur locally on the rock slopes, and alluvial and debris fans are developed at the outlets of incised rock gullies (Pearce et al., 2014). Scree is likely to have formed during periglacial conditions that existed during the retreat of the Late Devensian glaciers and in unglaciated areas during the Younger Dryas. However, the presence of active scree and debris cones indicates sediment production has persisted up to the present day. A range of dating evidence from across the wider Scottish Highlands, summarised by Ballantyne (2021), indicates that in general, gullying and fan development have occurred episodically throughout the Holocene, with local influence from historic human activity as well as climatic conditions including extreme rainfall events.

Mass-wasting processes on steeper inner-valley slopes include debris flows associated with bedrock gullies and debris avalanches on regolith-covered (colluvial) slopes (following the classification of Hungr et al., 2013), as well as rock slope failures (RSFs). In the Gameshope catchment, a comparatively large RSF occurs in the eastern valley slope (Pearce et al., 2014). Following the classification of Jarman and Harrison (2019), the RSF is a rockslide with a short travel distance between the prominent back scarp and the deformed rock mass below. RSFs in the study area are paraglacial landforms resulting from deformation associated with

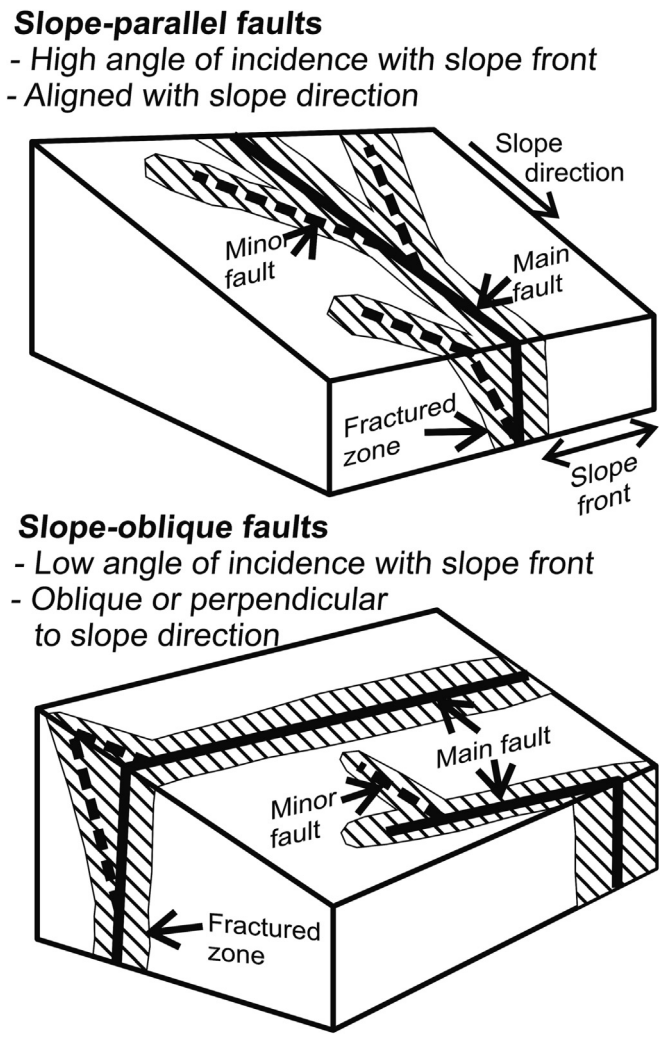

Fig. 2. Schematic illustration of contrasting fault–slope relationships in the study area. All fault planes in the area are sub-vertical to steeply dipping. Faults are described according to the trend of the fault with respect to the plane of the slope. Where faults trend sub-parallel to the slope direction (*i.e.,* the direction of maximum dip of the slope), they are termed 'slope-parallel', and where faults trend oblique or sub-perpendicular to the slope direction they are termed 'slope-oblique'.

multiple episodes of glacial erosion and loading/unloading (*cf.*, Jarman and Harrison, 2019; Ballantyne, 2021).

3. Methods

3.1. Geomorphic mapping

The study area includes slopes with contrasting fault–slope geometries allowing for comparative analysis of the geomorphic features and processes associated with these structures (Fig. 2). In the Codleteth catchment (Fig. 1, Area A), the main fault trend is sub-parallel to the slope direction. In the lower section of the catchment of the Games Hope Burn (Fig. 1, Area B), the western slope is bisected by several faults that are oblique to the slope direction, whilst the eastern slope is unfaulted.

Geomorphic mapping of the slope deposits and landforms was undertaken at 1:2000 scale using aerial photograph and digital elevation model (DEM) analysis and field mapping. Data used included the following national-coverage datasets: Aerial Photography for Great Britain (APGB) aerial imagery at 25 cm resolution (APGB © Getmapping Plc, Bluesky International Ltd.); the APGB 2 m Digital Surface Model (DSM, APGB © Getmapping Plc, Bluesky International Ltd.); and the Bluesky 5 m Digital Terrain Model (DTM, version 1.5, 2020 © Bluesky International Ltd.). Mapped features include landforms and deposits related to glacial erosion and deposition (inner valleys, till, morainic deposits), post-glacial rock slope failures, periglacial slope processes (solifluction deposits), and postglacial slope and alluvial processes (gullies, debris cones and debris aprons, colluvium and alluvial fans).

Landforms related to postglacial erosion and transport of slope material are of particular significance as sediment source areas. These include features associated with debris avalanches on open slopes, where vegetated hollows mark relict backscarp areas and transport paths, and debris flows occurring within confined gullies. These gullies are long-lived erosional features formed as steep-sided linear bedrock channels that are cut into valley-side slopes. These form individual linear features tens to hundreds of metres in length as well as complex networks.

General information on the nature of the superficial deposits was derived from field observations of surface exposures and sections, and from quantitative analysis of field photographs. The latter was limited to selected locations that were not obscured by vegetation cover.

3.2. Fault mapping and fracture density

A detailed fault map for the area at 1:2000 scale was constructed from field observations of fault rock and fault-breccia (Fig. 1), linked to mapping of slope landforms, including hollows and breaks-in-slope, from aerial photography imagery and DEM datasets. Spatial variation in fracture density associated with the mapped faults was determined by quantitative analysis of scaled outcrop photographs at 52 locations (Fig. 1). Outcrop locations were selected, where possible, to ensure representative analysis of variation in fracture density within the site area. Fracture density for each site was derived from digitised fracture networks captured for circular sampling windows following the method of Palamakumbura et al. (2020) (Fig. 3). Areal fracture density values were calculated by measuring the average fracture length per unit area (m/m^2; Singhal and Gupta, 2010), from fracture networks digitised within one to three circular windows. The circular windows were placed to avoid overlap, with placement constrained by the outcrop shape. Window size was also scaled to the outcrop width and degree of fracturing to ensure appropriate image resolution for delineating the fracture networks, with the radius ranging from 0.1 m for the highest fracture densities to 0.5 m for low fracture densities (78 % of all fracture windows were 0.25 m radius, 14 % 0.5 m, 9 % < 0.125 m).

Estimates of block size, where blocks are defined from 2D outcrop images by the intersection of fractures in rock outcrops, were made

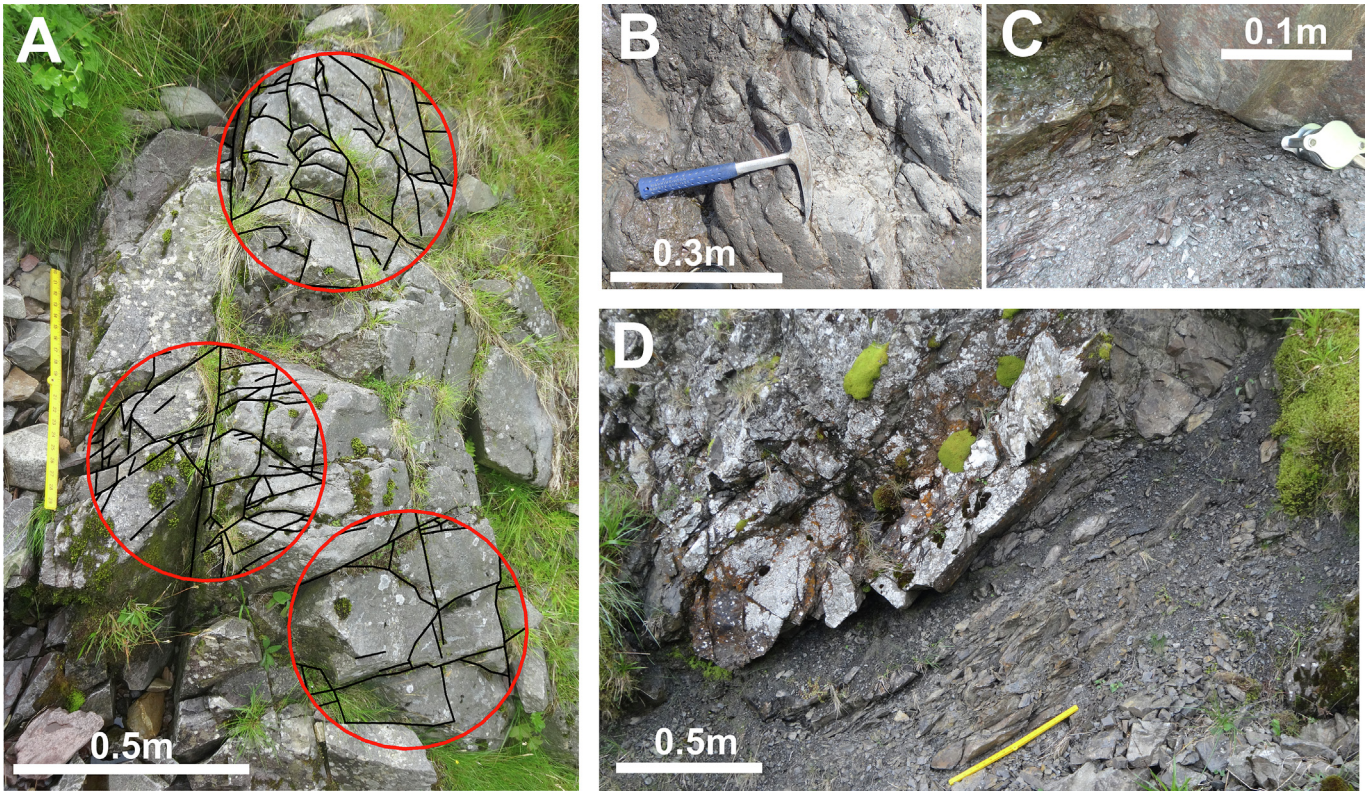

Fig. 3. Images of faulted and unfaulted wacke sandstone from the study area. A: Unfaulted sandstone showing circular windows (red circles) and digitised fracture measurement linework (black lines). B: Cataclasite exposure in the Codleteth Burn. C: Highly comminuted sandstone in a fault zone near the Codleteth Burn. D: Part of a fault fracture zone exposed in a gully in the western slope of the Gameshope Catchment.

for selected sites covering a range of fracture densities to establish a relationship between the fracture density and the size of blocks being sourced from bedrock into the slope sediment system. Block size was estimated using the circular window as a sampling area for delineation of coherent blocks that intersect the window, with the block diameter taken as the long axis of the block (Fig. 4). The method reflects a hybrid digital approach combining fracture analysis (Palamakumbura et al., 2020) and grain-size analysis (*e.g.*, Neely and DiBiase, 2020) based on image interpretation conducted in a standard GIS package.

3.3. Sediment coupling

A qualitative approach to evaluating slope-to-stream coupling relationships in gully networks was applied to focus areas including the Codleteth catchment (Fig. 1, Area A) and a sub-area of the Gameshope catchment (Fig. 1, Area C). Gully networks were recorded as coupled, partially coupled or uncoupled with respect to the slope foot — occupied by the Talla Water and Talla Reservoir (Area A), and the Games Hope Burn (Area C). The designation follows definitions and typologies provided by Fryirs et al. (2007), and Fryirs (2013).

The proportion of sediment removed post-glacially was determined from the balance between excavated gully and deposited alluvial fan volumes for the regions covered by Areas A and C in Figure 1. The volumes were estimated by constructing a synthetic 'pre-gully' ground surface using ARC GIS geoprocessing tools and subtracting the modern DTM from this synthetic surface following a process adapted from the method of Carter et al. (2020). Due to the narrow nature of the gullies and associated fan deposits in Area C (Gameshope), the synthetic pre-erosion ground surface was derived simply by clipping the gullies out of the APGB DTM and re-interpolating using a Natural Neighbour interpolation. For Area A (Codleteth Burn), a synthetic pre-erosion surface for the larger gully area was constructed by extending contours from the slopes adjacent to the gully. These synthetic elevation contours were used to constrain points at 20 m spacing which were integrated with the clipped DTM and re-interpolated using the Natural Neighbour algorithm.

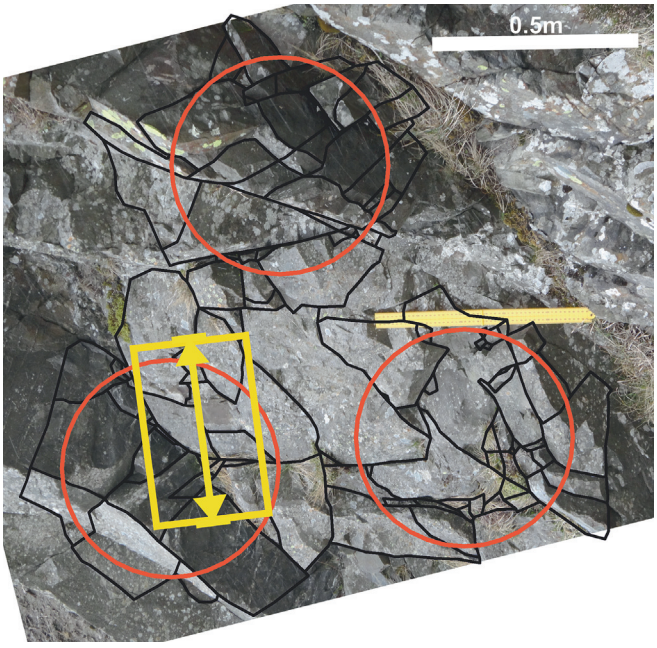

Fig. 4. Image of a wacke sandstone outcrop showing the blocks formed by the fracture networks (black lines). Long axes of all complete blocks intersected by the circle were measured as the longest side of a bounding box (yellow box and arrow).

3.4. Sediment connectivity

In addition to the qualitative assessment of coupling relationships, sediment connectivity was quantitatively assessed using the index of connectivity (IC) developed by Borselli et al. (2008) with the additional topographic weighting factors of Cavalli et al. (2013). IC is a function of the catchment area and distance along the flow path estimating the likelihood that any particular part of a catchment will supply sediment to a specified 'sink' (*e.g.*, a river channel, lake or reservoir). It is defined as the ratio of upslope and downslope functions that describe the likelihood that material will be sourced from an upslope catchment area (D_{up}), and the likelihood that sediment will pass along a flow path to the specified sink (D_{dn})

$$IC = \log_{10}\left(\frac{D_{up}}{D_{dn}}\right) \tag{1}$$

where D_{up} is a function of the mean slope ($\overline{S}$) and area (A) of the upstream source region:

$$D_{up} = \overline{W}\overline{S}\sqrt{A} \tag{2}$$

$\overline{W}$ represents a weighting factor related to topographic roughness, which affects the efficiency of supply and transport (Cavalli et al., 2013). The potential for sediment to pass from a point to the defined sink (D_{dn}) depends on the distance (d_i) that the sediment must move along the flow path:

$$D_{dn} = \sum_i \frac{d_i}{W_i S_i} \tag{3}$$

where W_i and S_i are, respectively, the weighting factor (W) and slope (S) of the ith cell. Sediment connectivity analyses were run in ArcGIS 10.7.1, using the Bluesky 5 m Digital Terrain Model (DTM). To assess hillslope to channel coupling, the main streams of the Talla Water and Games Hope Burns, and the Talla reservoir were taken as the sinks.

An additional geological weighting factor (G) to account for the impact of faulting on the rock mass was also calculated from empirical data gathered in this study (Section 5). The geological conditioning affects both the availability of material for erosion, and the grain-size of the sediment entering the slope–sediment system. Hence, it affects both the upslope and downslope components of the index. The influence of fault orientation is not included in the function as it is implicit in the spatial application of the model *i.e.*, the spatial distribution of G with respect to the topographic parameters. The revised formulation of Eq. (2) is

$$D_{up} = \overline{GWS}\sqrt{A} \tag{4}$$

where $\overline{G}$ is the geological factor reflecting enhanced erodibility and reduced grain size. Eq. (3) becomes

$$D_{dn} = \sum_i \frac{d_i}{S_i W_i G_i} \tag{5}$$

where W_i is the roughness factor and G_i the grain-size factor for each cell.

The intention of this analysis is to demonstrate the impact of faulting on sediment systems where *in situ* fractured bedrock is the key source material. A relatively thin layer of superficial deposits is present overlying bedrock across much of the area. However, much of this sediment comprises colluvium and talus derived from bedrock through post-glacial weathering and slope processes and is therefore part of the system of processes reflected by this formulation of connectivity. It should be noted that IC is formulated for water-mediated flows and does not fully account for factors affecting rockfall–talus systems. Localised glacial deposits including moraines and thin till

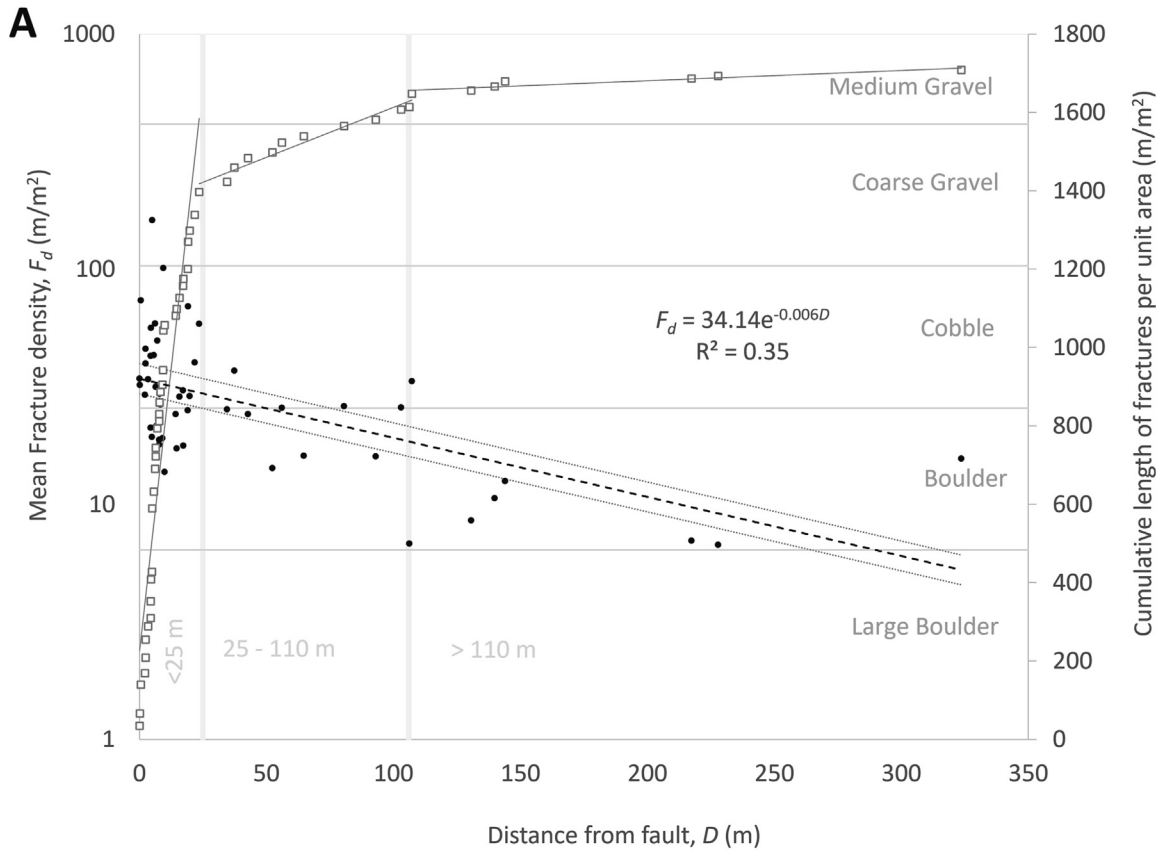

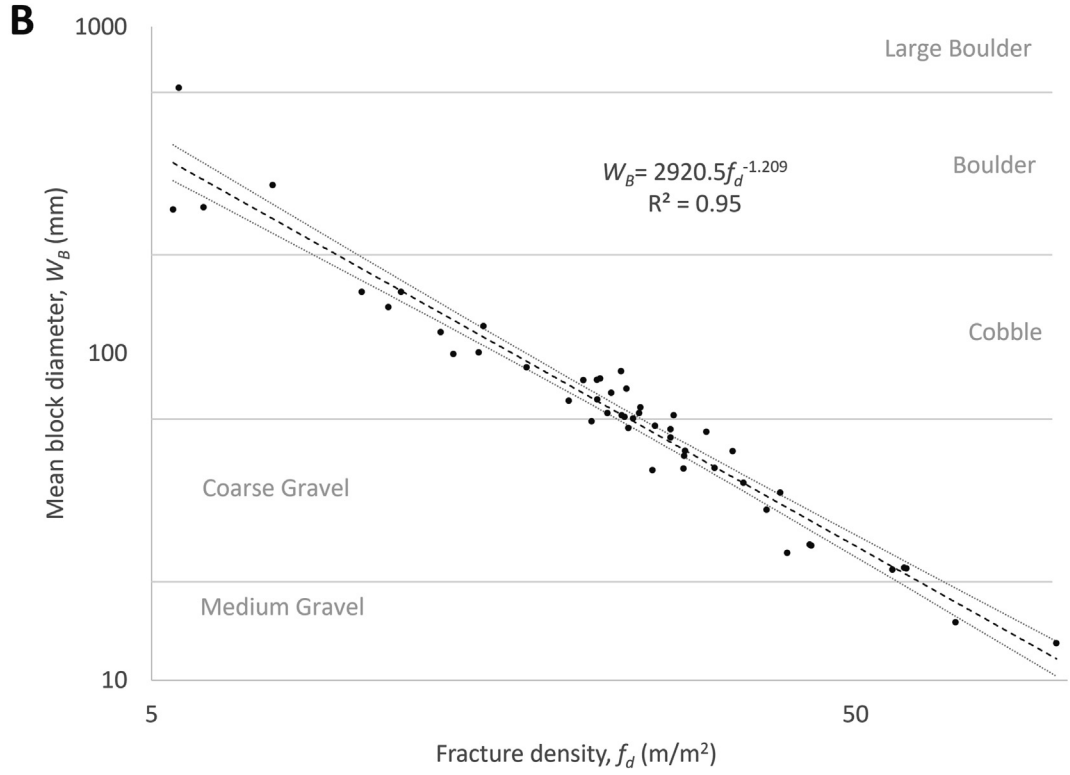

Fig. 5. Characterisation of fault-related fracture density. A: Relationship of mean fracture density (F_d), calculated from multiple sampling windows at each outcrop location, to distance from a mapped fault structure (D) (black circles). The logarithmic regression (dashed black line) is significant $p < 0.01$, with 95 % confidence interval (dotted grey lines). The cumulative length of fractures per unit area (white squares) was derived as sum of mean fracture length with increasing distance from the fault. Distance thresholds at approximately 25 m and 110 m are used in subsequent discussion of fault proximal (<25 m), marginal (25–110 m) and distal (>110 m) zones. B: Relationship of measured fracture density (f_d) and mean block diameter (W_B) calculated for individual sampling windows at selected sites chosen to cover a range of fracture densities. The grain-size thresholds shown have been calculated based on the ISO 14688-1 grain-size scale. The empirical relationship of W_B to f_d has been used to calibrate F_d for grain-size on plot A.

cover are not accounted for in this analysis as they occur only sparsely within the study area and are generally restricted to the slope base and valley floor. Periglacial deposits and blanket peat on upland plateaus are likewise excluded.

4. Results — faulting and slope process systems

4.1. Fault characterisation

The faults mapped in the study area comprise a network of structures orientated generally north–northeast (NNE) to south–southwest (SSW) (Fig. 1). In Area A, the fault network comprises a main (central) NNE–SSW trending fault, with a series of minor splays at high angles of incidence. In Area B, a set of sub-parallel NNE–SSW trending faults run oblique to the western slope of the Gameshope valley. Within the sub-area covered by Area C, minor transverse faults occur between adjacent NNE–SSW trending structures (Fig. 1). These accommodate displacement along the main faults and may be associated with transfer of displacement to adjacent parallel NNE–SSW trending faults.

The locations of measurements of average fracture density (F_d) derived for the 52 outcrops range from <1 m to 324 m horizontal distance from a mapped fault. F_d values range from 4.7 m/m^2 to 161.6 m/m^2, with a mean of 32.8 ± 3.6 m/m^2. The fracture density shows high variability, particularly in areas within approximately 25 m of the fault zone, but generally decreases with increasing distance from the fault (Fig. 5A, regression $p < 0.001$).

Three zones of deformation with respect to distance from the fault are interpreted based on breaks in slope of the cumulative fracture length curve (*cf.*, Choi et al., 2016) and the observed variability of F_d with distance in Figure 5A. A proximal zone within 25 m of a mapped fault yields a mean F_d of 39.9 ± 4.8 m/m^2 ($n = 35$, ±standard error), a marginal zone between 25 and 110 m from a fault yields a mean F_d of 22.8 ± 2.6 m/m^2 ($n = 11$), and a distal zone over 110 m from a fault has a mean F_d of 10.2 ± 1.4 m/m^2 ($n = 6$). Mann–Whitney *U* tests indicate that the mean F_d values for each zone are significantly different ($p < 0.05$).

The coefficient of variation of F_d calculated for the proximal zone (70.9) is higher than for the marginal and distal zones (38.5 and 34.1 respectively), reflecting the high variability in fracture density observed close to the faults. This is consistent with a fault system in which greater deformation is partitioned into narrow zones surrounding less deformed wedges or slivers of rock (*e.g.,* Fig. 3D).

Fracture density is strongly inversely correlated with *in situ* block diameters derived from the spatial intersection of fractures within the network (Fig. 5B). The empirical relationship of block diameter to fracture density was used to calibrate a rough spatial variation in the grain size of fractured bedrock source material (Fig. 5A). In the proximal zone the dominant grain sizes indicated by the fracture density range from boulder to coarse gravel, whereas in the marginal zone grain-size is predominantly boulder to cobble; in the distal zone clasts of boulder size are dominant.

The number of blocks calculated using selected sampling windows ranges from less than 10/m^2 for fracture densities lower than 8 m/m^2 up to approximately 2700/m^2 for fracture densities greater than 70 m/m^2. Thus, the results confirm that faults in the study area are associated with zones of increased fracture density, resulting in the conditioning of potential source material such that bedrock close to the fault will yield more abundant, smaller clasts.

4.2. Unfaulted slope system

The eastern slope of the Lower Gameshope catchment is not bisected by fault structures (Fig. 1, Area B). The lower portion of the valley side slope falls into the marginal (25–110 m) zone adjacent to faults that follow the valley floor, but the bulk of the slope is in the distal zone (over 110 m).

The absence of faulting means that the main discontinuities in the rock mass are joints associated with near vertical bedding at 20–60 cm spacing striking between northeast–southwest and north–northeast to south–southwest (Fig. 6). The dominance of planar, bedding-related joints in unfaulted areas gives an anisotropic character to the rockmass (Fig. 7A and B). The eastern valley slope curves, with variation in slope aspect ranging from the northwest, in the north of the area, to the southwest in the south. Thus, the strike of the slope in the northern half of the area is aligned roughly parallel to the strike of the bedding-related joints, whereas in the south, the slope strike is roughly perpendicular to the strike of the bedding-related joints.

The variation in the angle of intersection of bedding with the slope gives rise to differences in slope character. Within the inner valley, the slope comprises an upper exposed rock face (Fig. 6, feature a) with a relict talus apron developed on the mid to lower slope (feature b). Along the exposed rock face in the northern part of the area, localised reversals in the dip direction of bedding and disturbance of soil on the downslope edge of joint-bound slabs indicate tilting and downslope 'ploughing' of joint-bound slabs (Fig. 7C; *cf.*, Ballantyne, 2001). The talus slope is largely vegetated but surface material indicates boulder-grade blocks in the lower slope (Fig. 7D), fining to cobbles in the mid to higher slope area.

A rockslide (feature d) is present on the inner edge of the valley curve. A single gully (feature c) links the upper slopes, above the inner valley limit, to the valley floor and a well-developed valley-floor fan is present at the gully outlet. There is no evidence of faulting within the gully or associated with the rockslide. However, it is possible that the lower section of the gully and the back-scarp of the rockslide follow secondary joint orientations orientated approximately northwest–southeast (*cf.*, Fig. 7A and B).

Towards the southern part of the area, south of the rockslide, an active talus apron is developed on the lower slope (feature e). This comprises largely cobble sized clasts and the ongoing slope activity is consistent with an apparent increase in fracture density associated with the intersection of the slope perpendicular to the strike of the bedding-related joints.

4.3. Faulted slope system — slope-oblique fault trend

The western slope of the lower Gameshope catchment is bisected by several slope-oblique faults following two main zones — an upper zone near the top of the inner valley and a lower zone in the lower to mid slope (Fig. 6). The presence of these faults means that most of the slope falls into the proximal and marginal deformation zones.

The slope is mantled in colluvial deposits comprising angular, medium to coarse gravel with cobbles (2–10 cm diameter) and rock exposure in open slope areas is rare (Figs. 6, 8, feature f). Disturbance of the colluvial deposits is evident at the slope toe, where scars of seepage failures are seen, and in the upper slope where undulating ground is indicative of relict debris avalanche scars (Figs. 6, 8, feature g).

Several erosional slope features are associated with the lower fault zone, in the extreme north and southern half of the area. These features include relatively shallow hollows and breaks-of-slope running obliquely down the valley side (Figs. 6, 8, feature h), and narrow, discontinuous gullies running directly downslope (Figs. 6, 8, feature j). The former are associated with the main north–northeast to south–southwest fault structures, whereas the latter are formed along the lines of minor transfer structures developed between sub-parallel faults. The steep, discontinuous gullies (feature j) commonly have small debris fans developed at their outlets in mid-slope areas (Fig. 6).

4.4. Faulted slope system — slope-parallel fault trend

The minor catchment of the Codleteth Burn lies on the north side of the Talla valley and comprises an active debris-flow gully system. In this area, the faults are aligned parallel or sub-parallel to the slope direction

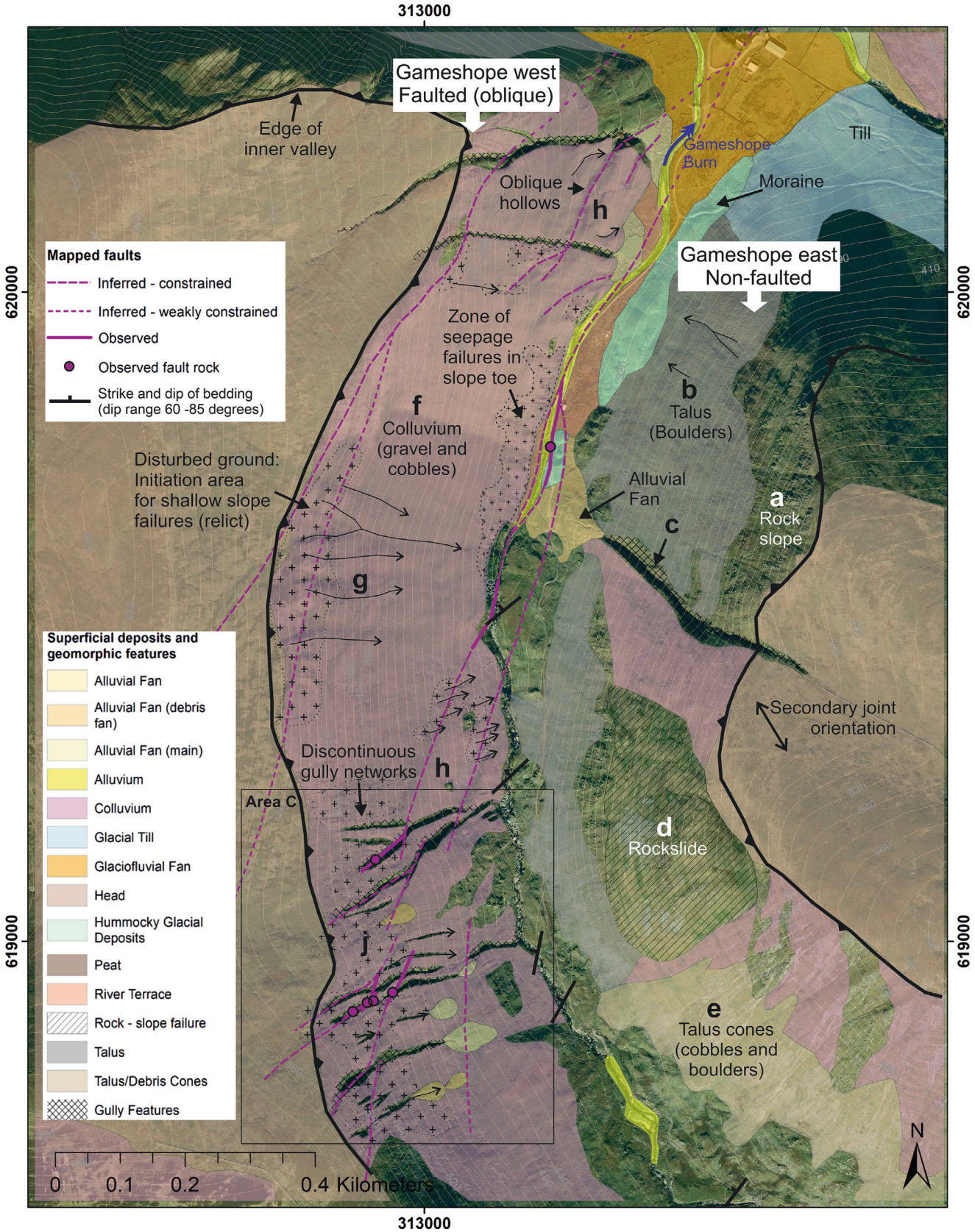

Fig. 6. Geomorphic map of the Gameshope area (Fig. 1, Area B). Features labelled with lower case letters are referenced in the text. Contains APGB aerial imagery © Getmapping Plc, Bluesky International Ltd. Ordnance Survey data © Crown copyright and database rights 2023.

(Fig. 9). Slopes adjacent to the steep gully are mantled in colluvial deposits (Fig. 9, feature l) which have been locally remobilised in debris flows forming minor fans and cones.

The steep Codleteth catchment comprises a branching network of deeply incised gullies which follow the strands and splays of the underlying fault network (Fig. 9, feature m). Within the gullies,

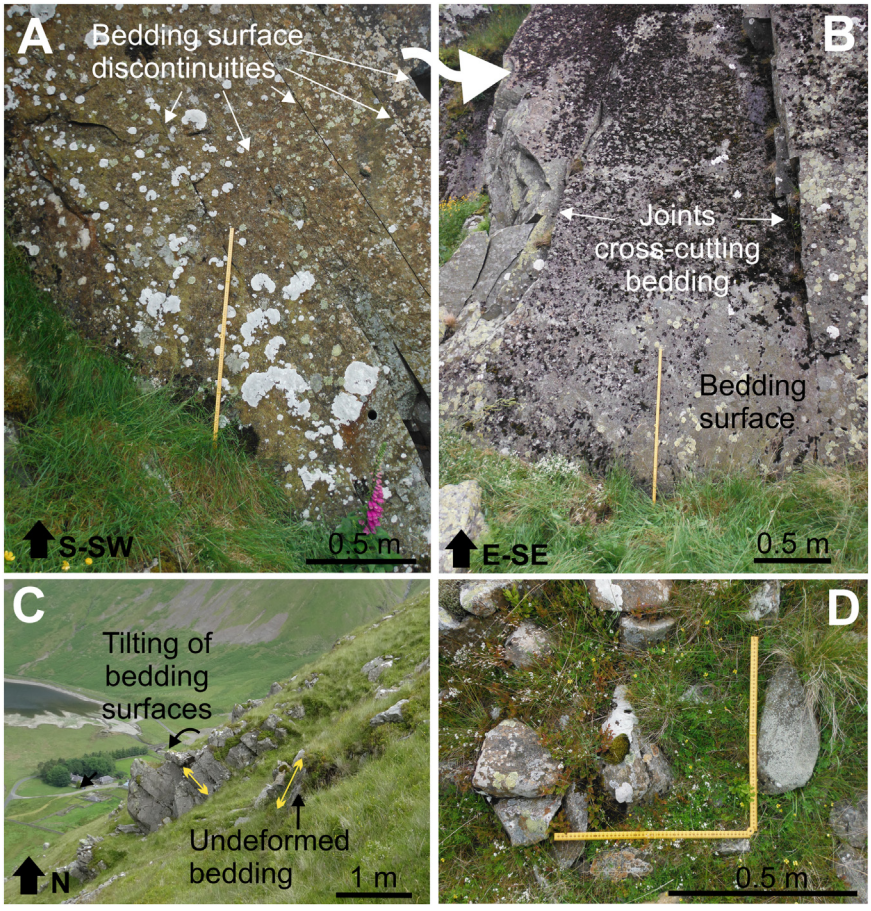

Fig. 7. Field images of unfaulted bedrock (A, B) and associated slope processes (C) and talus deposits (D) on the eastern slope of the lower Gameshope catchment. The rule is 1 m long.

upper rock slopes source debris material of coarse gravel to boulder grade into local talus cones which infill the narrow gullies and are periodically excavated and remobilised as debris flows (Figs. 9, 10A, feature k).

Debris flow deposits are present along the central gully and form a large alluvial fan system at the valley outlet (Fig. 9, feature n). The fan system comprises several generations of fan development, reflecting multiple phases of depositional activity and incision associated with progressive lowering and southwards propagation of the fan (Fig. 10A). The lowest fan level is currently active.

4.5. Slope angle and sediment process on open slopes

Mean slope angles for the east and west inner-valley slopes of the northern Gameshope catchment (Fig. 1, Area B) were derived from the slope of the APGB 5 m DTM. The unfaulted eastern slope has a mean slope angle of 35.71° ± 0.02, compared to the western slope which has a mean angle of 34.76° ± 0.03 (means are significantly different at $p < 0.001$). Histograms of the slope angle indicate that the faulted west slope has negatively skewed unimodal distribution with a mode at 37° (Fig. 11). This reflects a relatively constant slope angle with a uniform distribution of colluvial material. Low slope values are localised in the discrete hollows and breaks in slope associated with the oblique faults, but the highest slope values are associated with the toe of the slope, which has been steepened by seepage failures and undercutting by the Games Hope Burn. By comparison, the un-faulted eastern slope has a bimodal distribution of slope angle with peaks at 32° and 39°. This is associated with the presence of the steep rock exposures on the upper part of the slope (Fig. 6) and the lower angle talus-covered slopes developed in the mid and lower slope areas.

Although the aspect differs between the two sides of the valley, the differences in the nature of the deposits and sediment processes on the adjacent slopes are indicative of contrasting grain-size and

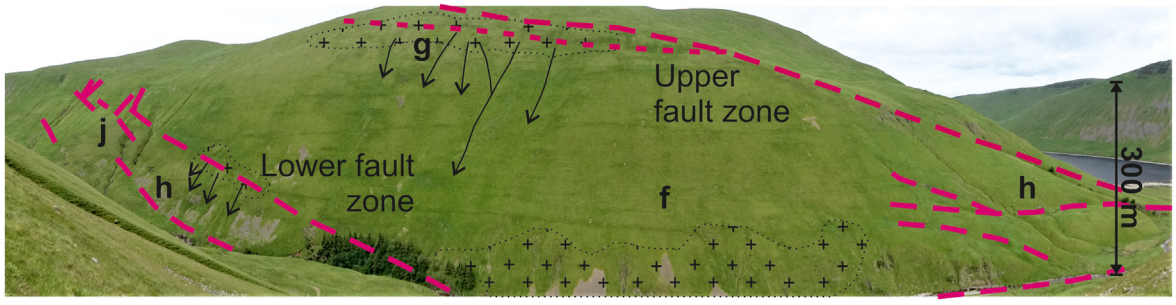

Fig. 8. Panoramic image of the western slope of the lower Gameshope catchment showing the organisation of slope features noted in Fig. 6.

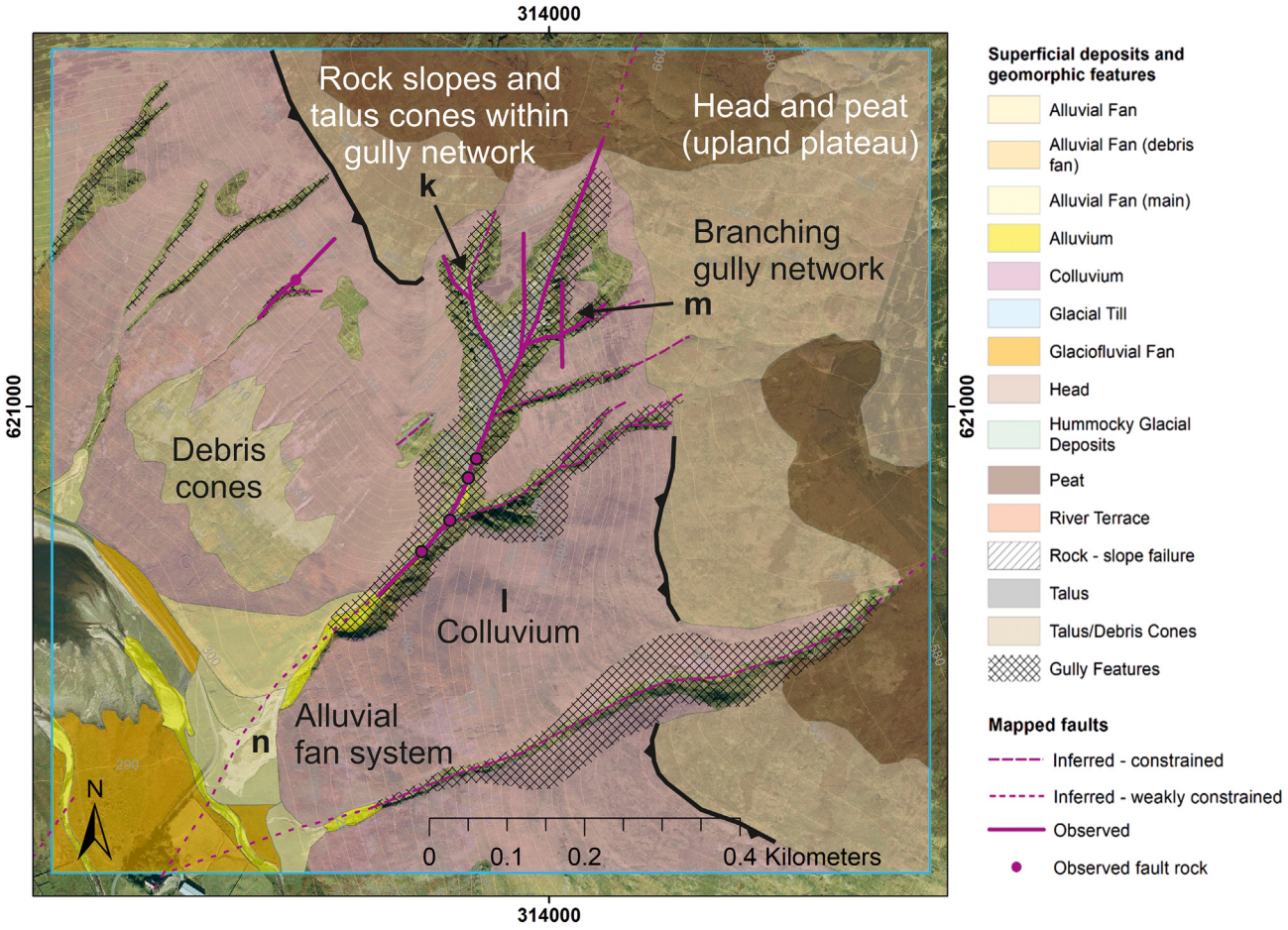

Fig. 9. Geomorphic map of Codleteth Burn area (Fig. 1, Area A). Features labelled with lower case letters are referenced in the text. Contains APGB aerial imagery © Getmapping Plc, Bluesky International Ltd. Ordnance Survey data crown ©Crown copyright and database rights 2023.

abundance of material derived from the source rock. The absence of coarse-grained, boulder-grade material in colluvial deposits on the western slope, along with the consistent slope, uniform colluvial cover and dominance of creep and debris avalanches (Fig. 8), is consistent with sediment supply from a relatively fractured source rock. By contrast, in the east, the rock-fall and tilting-sliding dominated processes of the upper rock slope, and the abundance of large boulders in the talus deposits are indicative of a sediment system conditioned by relatively sparsely fractured source rock.

5. Results — sediment coupling and connectivity

5.1. Influence of faults on slope — channel coupling

The primary processes for transporting sediment from slopes into the main streams and the Talla reservoir are debris avalanches occurring in open-slope areas and debris flows in gully networks. Due to the glaciated nature of the catchment, with a relatively broad valley floor, the gully networks are particularly important for mobilising and

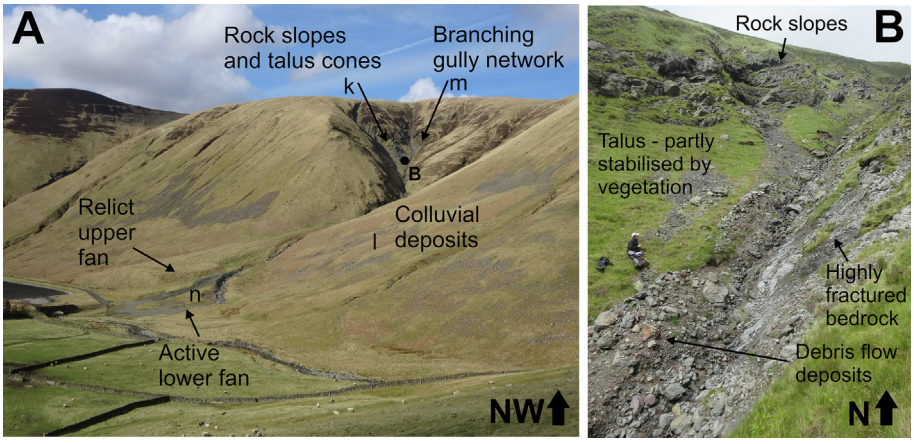

Fig. 10. Field photographs of the Codleteth Burn catchment (Fig. 1, area A). A: Overview of the catchment. The location of image B is indicated by the black dot. Letters refer to features identified in Figure 9 and discussed in the text. B: The upper part of the slope system within the gully network.

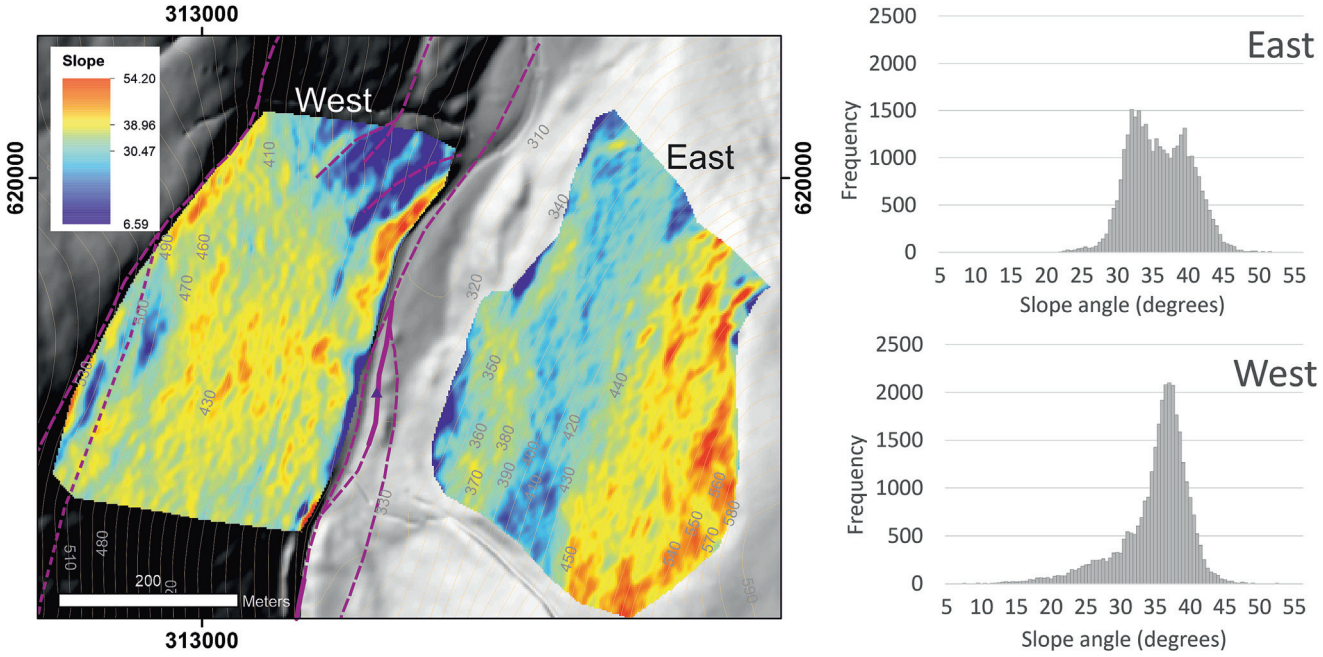

Fig. 11. Comparison of slope angle for the faulted west and unfaulted east slopes in the northern sector of the Gameshope area. Slope derived from the APGB 2 m DTM. Contains APGB aerial imagery © Getmapping Plc, Bluesky International Ltd.

transporting sediment into stream channels. Erosional gullies that are incised into bedrock are not unique to faulted slopes but they occur more frequently, or as more connected systems, in association with faults (Figs. 6 and 9). Alluvial fans are developed at the outlets of many gullies and reflect partial, and temporary, storage of sediment within the slope system.

A single gully is present in the unfaulted eastern slope system in the Gameshope catchment (Fig. 6) connecting the upper slopes above the inner valley to the valley floor where a small fan is developed at the gully outlet. No evidence of faulting was observed in the gully, however much of the channel is aligned along well-developed northwest–southeast orientated joints that intersect the bedding fractures (Fig. 6B). On the faulted slopes, gullies are formed in numerous areas in association with faults. Two main areas of gully formation, the Codleteth Burn (Area A), and the southern part of the western Gameshope slope (Figs. 1 and 6, Area C) are contrasted in Figure 12.

The gullies on the western side of Gameshope are relatively narrow and shallow, forming a discontinuous network. Short, steep gullies are developed along the transfer faults which are slope-parallel, but these commonly end, or are diverted where they intersect a main fault with a slope-oblique trend (Fig. 12A). The hollow or break-in-slope developed along the oblique fault disrupts the downwards flow path, in some cases resulting in deposition of minor mid-slope debris fans, in other cases diverting the flow along the oblique fault for a short distance before linking to a lower gully path.

By contrast, the Codleteth Burn catchment comprises a highly connected network of deeply incised gullies formed due to the coincidence of the fault alignment with the maximum slope angle, thereby enhancing the erosive potential of the system (Fig. 12B). The effectiveness of sediment transfer is indicated by the large valley-floor fan system, which has remained periodically active since deglaciation.

The volume of material removed from the gully systems, has been estimated by comparing the current DTM with a reconstructed immediately 'post-glacial' DTM surface. In the Codleteth Burn gully system (Figs. 9, 12B), approximately 4.8×10^5 m^3 of rock has been eroded from the gully, with approximately 1.3×10^5 m^3 stored in the fan at the valley outlet. This represents about 28 % of the material eroded from the gullies, with the remaining 72 % evacuated from the system into the Talla Water. Prior to the creation of the reservoir, the Talla Water flowed down the Talla valley towards the northwest to a confluence with the River Tweed. The total amount of rock eroded from the Codleteth Burn gully system equates to 131 m^3/m of fault length. In the west Gameshope gully system (Figs. 6, 12A), approximately 11.2×10^3 m^3 has been eroded, with 1.8×10^3 m^3 stored in mid-slope fan deposits, which is about 16 % of the material eroded from the gullies. The remaining 86 % of the eroded material has been evacuated along the Games Hope Burn. The rock eroded from the Gameshope gully system equates to 4.9 m^3/m of fault length.

5.2. Faulting and sediment connectivity

Standard connectivity indices use topographic parameters to compute the potential for sediment transport from slopes to sinks, highlighting areas of catchments that may yield enhanced sediment loads and may be particularly responsive to changing conditions (Fig. 13A; *e.g.,* Cavalli et al., 2013; Bollati and Cavalli, 2021). However, in addition to the topographic controls (*i.e.,* slope angle), geological constraints on sediment availability are also important in determining the spatial distribution of sediment source areas.

The connectivity index as estimated from topography alone underestimates the relative sediment generating capacity of the Codleteth Burn catchment in particular (Fig. 13A, Area A). To account for the spatial heterogeneity in fault-related fracturing an additional weighting factor is included to reflect enhanced sediment availability and reduced grain-size of source material in areas closer to faults (*G* in Eqs. (4) and (5); Fig. 13B). The weighting factor was calculated using the empirical relationship of fracture density and distance from a fault derived in Figure 5A and normalised to a 0–1 range. The introduction of the fault-weighting improves the correspondence between the sediment pathways predicted by the connectivity index and the observed sediment process systems, particularly in the region of the Codleteth Burn (compare Fig. 13A and C).

The connectivity index is also estimated for early 'post-glacial' times, *i.e.,* immediately after deglaciation, using the fault-weighting factor and a reconstructed topography prior to gully erosion (Fig. 13D).

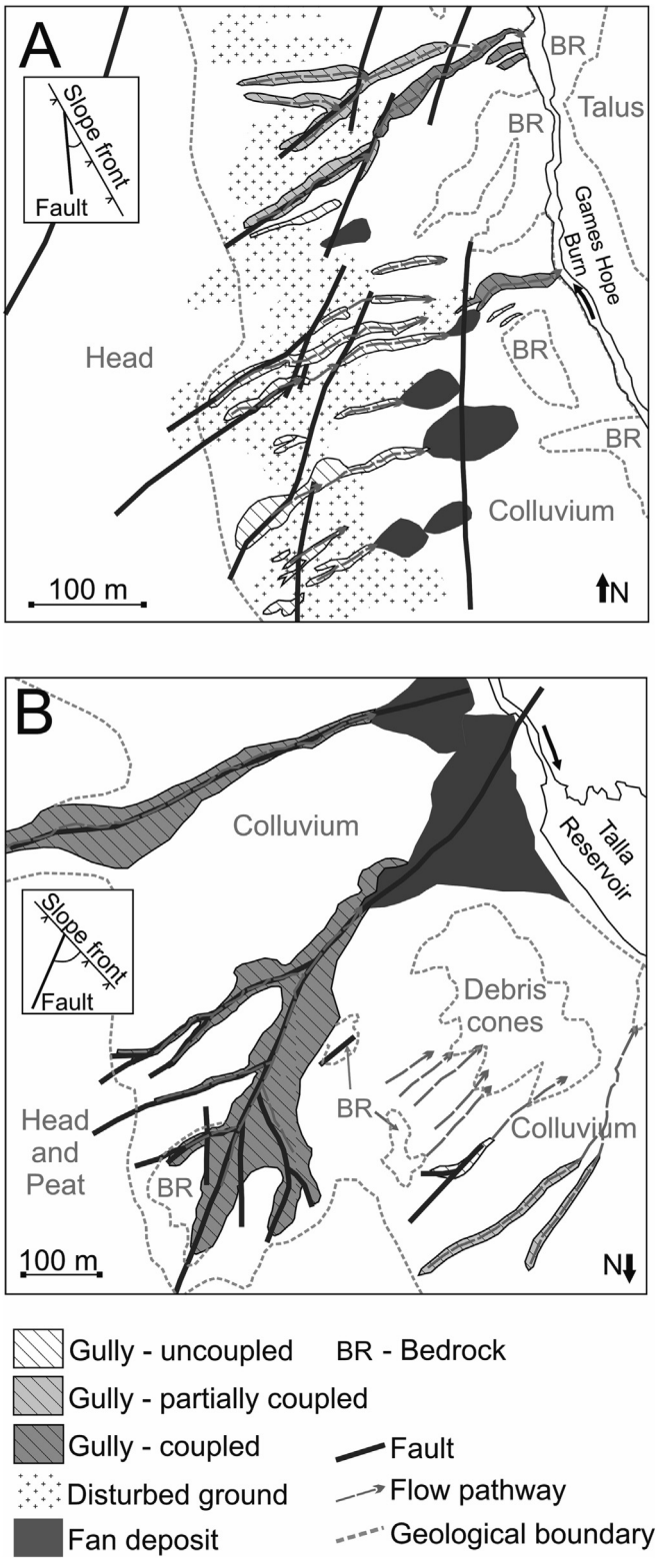

Fig. 12. Coupling/connectivity maps of selected areas in the southern part of (A) Gameshope (west) and (B) Codleteth Burn, contrasting the nature and continuity of gully development. The degree of coupling is assigned based on the observed connection of drainage pathways within the gully to the main stream on the valley floor (uncoupled = no connection, partially coupled = indirect or episodic connection, coupled = direct connection). The Codleteth Burn map is rotated with north towards the bottom of the page to allow easier comparison of the two systems.

Comparison of the modern and immediately post-glacial connectivity (Fig. 13C and D) highlights more focused areas of connectivity associated with the lower Codleteth Burn and the adjacent linear gully in Area A and is consistent with the formation of the alluvial fans at the outlets of both gully systems since deglaciation.

6. Discussion

6.1. Faulting, regolith production and 'source' material

Faults in the study area comprise linear zones of highly fractured rock. A link between areas of fractured rock and thicker regolith has previously been observed (Novitski et al., 2018). This is likely to arise due to higher rates of mechanical and chemical weathering associated with increased hydraulic connectivity through the fracture network (Owen et al., 2007; Novitski et al., 2018; Scott and Wohl, 2018). Our results show that the influence of this thicker regolith zone on the hillslope sediment system depends on the geometric relationship between the fracture zone and the slope.

Where faults are slope-oblique, thicker regolith forms in a belt traversing the face of the slope. In West Gameshope this occurs along two faults located in the middle to upper slope and the lower slope (Fig. 14B). It is likely that thicker regolith associated with the upper fault, which, in the northern part of the site, follows the upper edge of the inner valley, is a key source of material for the colluvial mantle that blankets the northern segment of the slope. By contrast, continuous spreads of colluvial deposits are absent from East Gameshope, where faults are not present. In the latter system, coarse boulder talus deposits occur below an upper rock-slope, with thinner colluvium only locally developed (Fig. 14A).

In the northern part of West Gameshope, disturbed ground and landforms associated with relict slope failures indicate that a number of debris avalanches (*sensu* Hungr et al., 2013) have occurred historically, in a linear zone contiguous with the upper slope-oblique fault (Figs. 6 and 8). The locus of avalanche initiation is consistent with conditions of enhanced sediment availability due to the presence of a thicker saprolite zone (*e.g.,* Brayshaw and Hassan, 2009) and the influence of increased groundwater flow (*e.g.,* Reid et al., 1997) (Fig. 14B). However, unlike the southern part of West Gameshope, the relict rock slope failures in the north are not associated with erosional gullies (*sensu* Brayshaw and Hassan, 2009). This may indicate that there are few slope-parallel transfer faults in the region, or that bedrock erosion along minor structures has been prevented by the presence of the thicker colluvial mantle sourced from the upper-fault band.

6.2. Fault orientation and the development of gully networks

Bedrock gully networks such as those in the study area are key elements in active sediment systems and need to be understood in order to mitigate debris-flow hazards and manage water and sediment fluxes affecting critical infrastructure (*e.g.,* Kondolf et al., 2014; Winter et al., 2016). The formation of gullies reflects the interplay between spatial and temporal patterns of surface run-off and groundwater flow, and the resistance of substrate to erosion (*e.g.,* Kirkby and Bracken, 2009). The results of this study illustrate the nature of this interplay by demonstrating how geological heterogeneity and slope form combine to control the form of bedrock gullies and gully networks.

The formation of gullies reflects positive feedback between enhanced erosion associated with the intensely fractured rock along the fault and the concentration of flow in topographic hollows. This feedback is enhanced where faults are more-or-less aligned with the direction of maximum slope. However, the development of the gully system also depends on the fault-network structure, in particular the continuity of faults in the slope-parallel orientation and the angle at which faults intersect (*cf.*, Molnar et al., 2007).

Discontinuous slope-parallel transfer faults such as those in the West Gameshope sub-area reveal local reductions in the slope of the gully thalweg at the point of intersection with the main oblique faults (Fig. 14C). Some of these intersections also occur at high angles between

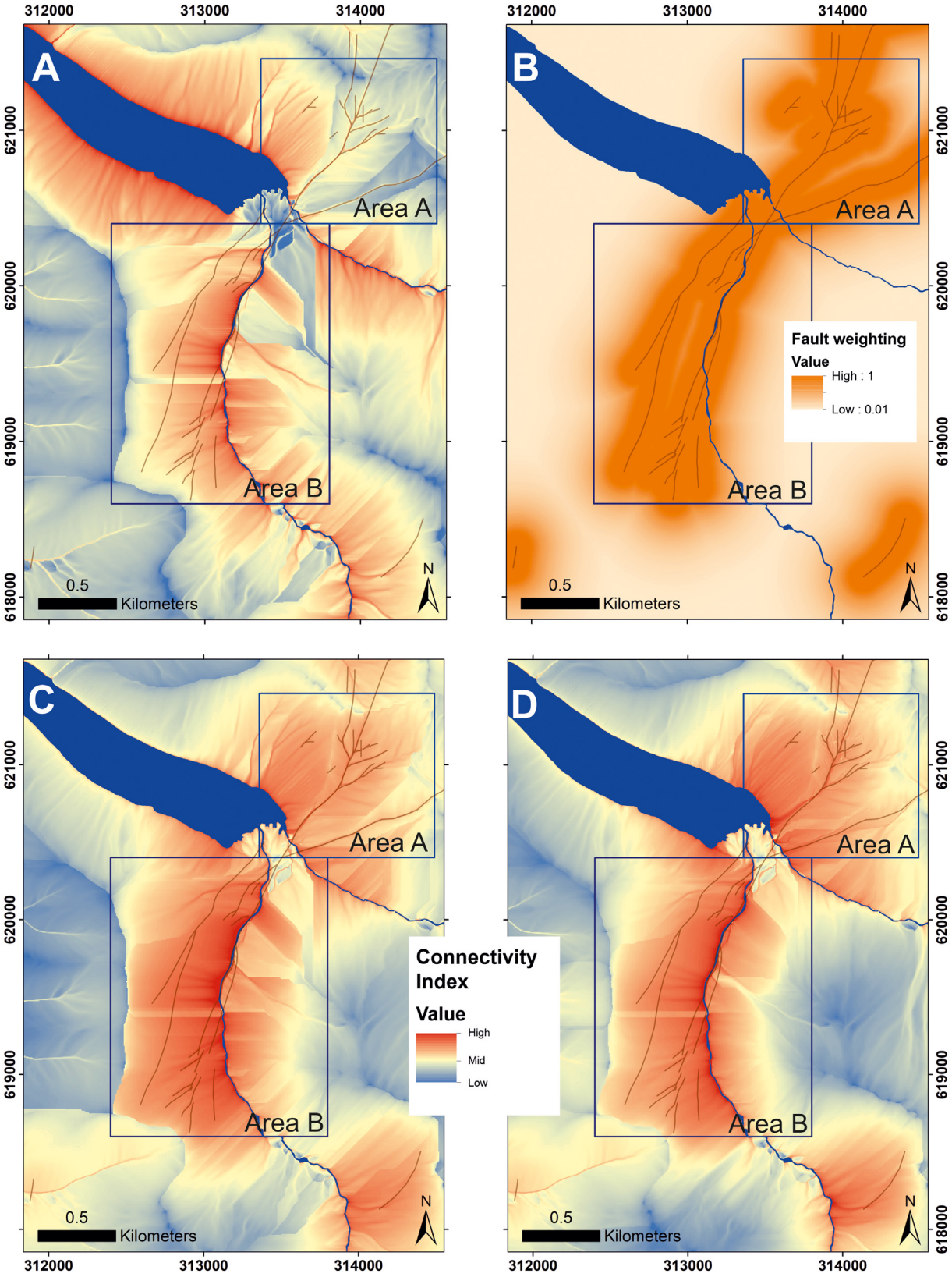

Fig. 13. Sediment connectivity indices (SIC) calculated for the study area. Sinks are shown in dark blue, namely the Talla Reservoir, Games Hope Burn and Talla Water. The boxed regions are Areas A and B (Fig. 1). The traces of mapped faults are shown as solid red lines. A: The SIC based solely on the topographic index calculated using slope and roughness weightings (Cavalli et al., 2013). B: Map showing the fault-conditioning weighting factor representing the empirical relationship of fracture density and distance from the fault as shown in Fig. 5A. C: The fault-weighted connectivity index calculated using the modern terrain. D: The fault-weighted connectivity index calculated using a reconstructed 'immediately post-glacial' DTM with gullies removed. This shows the potential for erosion and sediment connectivity accounting for faulting.
Derived from the Bluesky 5 m DTM © Bluesky International Ltd. Ordnance Survey data crown ©Crown copyright and database rights 2023.

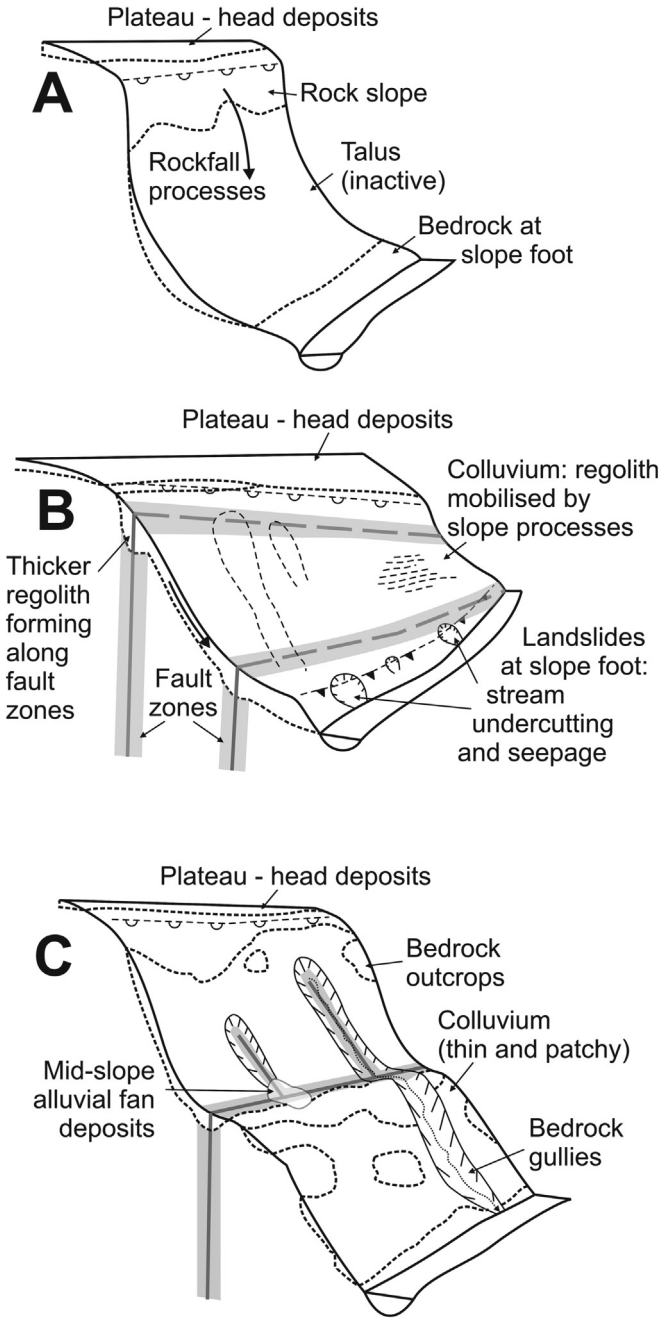

Fig. 14. Schematic diagrams showing the relationships between fault fracture zones and assemblages of deposits and geomorphic features along the inner valley of the Gameshope area (*cf.*, Fig. 6). The dashed line with semi-circle symbols marks the break in slope at the top of the inner valley. A: Unfaulted slope showing upper rock slope and lower talus slope. B: Slope-oblique faults showing thick colluvial deposits sourced from deeper regolith zones along faults. C: Slope-oblique faults with slope parallel transfer faults — note the absence of the upper fault which may account for thinner colluvial deposits present in this area. The thin colluvium would favour the development of erosional features including bedrock gullies and the rock bench along the mid-slope oblique fault system.

60 and 80°. In-gully deposition of debris flow material is more likely to occur where gully junction angles are greater than 65–70° (Benda and Cundy, 1990), and at points of reduced slope. Thus, the form of the West Gameshope fault network results in reduced erosion and enhanced deposition at fault intersections and a discontinuous and decoupled gully network. By contrast, gullies in the Codleteth Burn network display relatively consistent slope across confluences and intersection angles of less than 60°. Some in-channel deposition, including bars and levees associated with periodic debris flows is present within the system, but there is no evidence of internal 'buffering' (*sensu* Fryirs et al., 2007) of sediment transit within the system.

The influence of geological heterogeneity in controlling where gullies develop is likely to increase with the resistance of the intact bedrock. The study area comprises highly resistant, weakly metamorphosed and indurated wacke-sandstones with a strong contrast in strength between unfaulted and faulted rocks. However, in weaker or more highly jointed bedrock, gully networks may be less strongly influenced by discrete faults and fracture zones. Formation of bedrock gullies along linear structural weaknesses (faults and major joints) occurring parallel to slope has also been documented within small catchments in the European Alps (Loye et al., 2012) and in association with crater structures on Mars (Kumar et al., 2010). However, Burian et al. (2017) did not observe a direct link between faults and the spatial distribution of bedrock gullies in a study area in Slovakia. Their study region comprised sedimentary rocks of Neogene age including alluvial channel (sandstone) and floodplain deposits (mudstone and siltstone of the Volkovce Formation), as well as lacustrine and deltaic units. These strata have not been metamorphosed and are comparatively weak (Kovac et al., 2011); the lack of a link to faulting is consistent with climate, topography and land use factors playing more dominant roles in determining the distribution and form of gullies at the hillslope scale in a weak bedrock domain.

6.3. Controls on sediment storage within gully networks

Different patterns of sediment storage in the West Gameshope and Codleteth Burn gully networks may be associated with differences in the slope coupling to the valley floor, and consequently the amount of sediment entering streams and reservoirs (Fryirs, 2013). The strongly coupled gully network of the Codleteth Burn (slope-parallel fault system) is linked to a substantial outlet fan on the valley floor, whereas the discontinuous gully network of West Gameshope (slope-oblique fault system) is associated with multiple, small fan deposits formed in mid-slope areas. The total volume of sediment exported per metre of fault length from the Codleteth Burn system is over 20 times greater than that exported from the West Gameshope network, emphasising that the gully network developed along slope-parallel faults is a much larger sediment source.

Despite the enhanced coupling within the gully network, the Codleteth Burn system, which includes the large outlet fan, has a higher storage ratio (28 %) relative to the distributed gully system in West Gameshope (16 %). The lower storage ratio for the West Gameshope area likely reflects the lower abundance of sediment within the discontinuous gully network. Firstly, the thinner, smaller spreads of sediment associated with the West Gameshope gullies are likely to be less accurately identified and quantified and the volume of sediment deposits may therefore be under-estimated. Secondly, the small deposits located in mid slope areas are more likely to be mobilised and redistributed by diffusive processes such as slope wash and creep. Thirdly, the absence of valley-floor fan deposits at the lower gully outlets in West Gameshope likely reflects efficient removal of sediment by the Games Hope Burn, which runs in a steep bedrock channel with no adjacent flood plain in this area of the catchment (May and Gresswell, 2004). Thus, there is no accommodation space for sediment storage, and high transport capacity in the main-stream at the point of gully-stream coupling, resulting in the efficient evacuation of the gully-derived sediment that reaches the valley floor. Sediment mobilised by the Games Hope Burn will have been reworked downstream into the alluvial terraces and alluvial fan deposits of the lower Gameshope catchment.

By contrast, in the Codleteth Burn system, sediment has been concentrated in a substantial outlet fan deposited over a broad, flat plain of alluvial and glaciofluvial sediments at the head of the Talla valley (Fig. 9). This fan system reflects the greater accommodation space and lower transport capacity of the Talla Water at the point of gully–stream coupling, as well as the high volume of sediment supplied from the gully

network (May and Gresswell, 2004). Terracing of the fan, and erosion of the fan toe (Figs. 9 and 10), indicates partial reworking of sediment by the Talla Water in earlier post-glacial times.

6.4. Applications for connectivity analysis

The study shows that modification of a well-known and widely used connectivity index to account for the presence of faults gives better correspondence between the modelled pattern of sediment connectivity between slopes and streams and observations of erosional debris flow activity. This reflects the fact that spatial heterogeneity in rock properties arising from brittle faulting is a particularly strong conditioning factor for erosion and sediment transport due to the reduction in internal cohesion, increased water flow through the rock mass, and creation of smaller particles that can be more readily transported away from source areas (Roy et al., 2016; DiBiase et al., 2018; Scott and Wohl, 2018; Neely and DiBiase, 2020). The modification of the connectivity index (IC) in this study was formulated to reflect both the increased susceptibility of erosion and the increased mobility of clasts sourced from faulted bedrock. In principle, the methodology can be upscaled for wider application, particularly in metasedimentary terrains comparable to the study area. However, further testing of the empirical relationship of fracture density and distance from fault derived in this study would be needed.

It is likely that ignoring spatial variation in source material properties is a factor underlying previously observed mismatches between geomorphic observations of coupling and decoupling and sediment connectivity predictions in upland settings (Messenzehl et al., 2014). In recent work, Bollati and Cavalli (2021) indirectly accounted for the control exerted by geological factors through comparative geomorphological and sediment connectivity analysis of a catchment characterised by two distinct lithological domains, highlighting the importance of combining these approaches to understand system dynamics. This study demonstrates how a relatively simple geological metric can be directly incorporated into the formulation of IC, resulting in a model which better reflects the observed partitioning of erosion and sediment delivery from hillslopes to rivers and reservoirs.

Uplands are sensitive to land-use and climatic change (Bonn et al., 2009), and present a range of challenges for the management of water, energy and transport infrastructure (Winter et al., 2016; Finlayson, 2020; Palamakumbura et al., 2021). In these settings, sediment connectivity methods may offer real potential as tools for understanding system dynamics and informing effective environmental management and land use decision-making. To realise this potential, it is important that rock fracturing and lithological variability, as well as understanding of the complex grain-size controls on sediment cascades (Neely and DiBiase, 2020), are accounted for and sediment connectivity indices adequately reflect the dynamics of bedrock-dominated hillslopes.

Application of connectivity indices in decision-making would also benefit from targeted investigation of the links between connectivity and channel morphodynamics. Sediment delivery from hillslopes to rivers in upland landscapes is typically episodic and can locally affect the channel planform (*e.g.,* Harvey, 1991) and influence downstream changes in sediment grainsize within catchments (*e.g.,* Sklar et al., 2020). The influence of geology on spatial variation in sediment supply and grain size, as highlighted by this study, is therefore likely to exert an important control on river morphology and processes over a range of spatial scales. Future investigation of the relationship between the index of connectivity and channel morphodynamics would be valuable for decision-making and management applications.

6.5. Implications for landscape evolution

The study area lies within a post-orogenic terrain located in a passive-margin setting. Within Scotland, regional fault systems were formed and reactivated during several orogenic and extensional tectonic phases throughout the Phanerozoic but the current stress regime is low (*e.g.,* Woodcock and Strachan, 2012; Gordon and Stone, 2021), and glacio-isostatic adjustment is largely responsible for driving regional uplift (Firth and Stewart, 2000). The results of this study highlight how inherited fault-related deformation of the rock mass controls local erosional and depositional processes on slopes, with implications for long-term landscape evolution.

In the study area, post-glacial erosion is inhibited along valley sidewalls that are unfaulted or intersected by slope-oblique faults. By contrast, erosion along slope-parallel faults, as seen in the Codleteth Burn catchment, may ultimately lead to the formation, and persistence, of valleys over geological timescales (*e.g.,* Twidale, 2004; Manjoro, 2015; Scott and Wohl, 2018). The role of geological control on valley formation has been demonstrated in northeast Scotland, where the orientations of valleys within granitic rocks of the Cairngorms massif are controlled by linear alteration zones (zones of weakness caused by hydrothermal alteration around fractures) (Hall and Gillespie, 2017; Thomas and Gillespie, 2004). These structurally controlled valley systems have persisted since Devonian times and retain a strong imprint on the landscape despite regional uplift and tilting of the Scottish Highlands during the Cenozoic and periods of glacial and periglacial erosion during the Quaternary. A comparable assessment of potential structural control on the larger-scale valley systems of the Southern Uplands is beyond the scope of this study. However, our observations show how faulting is controlling the locus of erosion along the side walls of glacially scoured inner valleys, highlighting a key mechanism underpinning the evolution of this landscape.

7. Conclusions

Fault-related fracturing is a key control on post-glacial slope evolution in the study area. Faulted and unfaulted areas display different geomorphic patterns of postglacial sediment production due to heterogeneity in the abundance of source material, the mobility of clasts with respect to motion in water mediated flows, and the stability of slopes.

Because faults are generally linear features, the angle at which they intersect slopes within a catchment is a key control on the evolution of the slope–sediment system. The degree of alignment of the fault structure with the direction of maximum slope is a critical factor determining the degree of coupling between slopes and the valley floor. Close alignment of the fault trend and the direction of maximum slope results in higher erosion rates, and higher levels of coupling in debris flow systems.

By contrast, faults with slope-oblique trends are associated with more restricted erosional debris flow activity and reduced coupling. However, the efficacy of sediment transfer to the valley floor may be reduced in circumstances where fault trends are aligned with the slope direction and large fans form at the outlet of highly connected gully systems. This observation highlights a feedback response associated with the complex dynamics of sediment storage within glacially-conditioned mountain landscapes.

Accounting for faulting-induced heterogeneity in the erodibility and mobility of source material improves the correspondence of sediment connectivity models with observed sediment dynamics within the catchment. Simple weighting factors to account for source material heterogeneity may be readily adapted to account for other sources of variability in geological material properties, such as tensile strength. Hence this approach provides a useful way of adapting sediment connectivity models for use in a range of bedrock-dominated systems. Ensuring that sediment connectivity models accurately reflect real-world systems is necessary to support their use for informing the planning and management of upland infrastructure.

Declaration of competing interest

The authors declare that they have no known competing financial interests or personal relationships that could have appeared to influence the work reported in this paper.

Acknowledgements

The authors would like to thank Jonathan Lee for supporting the work and providing valuable feedback and discussions, and Romesh Palamakumbura for preliminary review and feedback. BGS authors publish with the permission of the Executive Director of the British Geological Survey (UKRI).

Funding sources

The work was funded as part of NERC National Capability activities.

References

Ballantyne, C.K., 2001. Measurement and theory of ploughing boulder movement. Permafrost and Periglacial Processes 12, 267–288. https://doi.org/10.1002/ppp.389.

Ballantyne, C.K., 2021. Upland landscapes and landforms of the southern uplands. In: Ballantyne, C.K., Gordon, J.E. (Eds.), Landscapes and Landforms of Scotland, World Geomorphological Landscapes. Springer, Cham https://doi.org/10.1007/978-3-030-71246-4_27.

Benda, L.E., Cundy, T.W., 1990. Predicting deposition of debris flow in mountain channels. Canadian Geotechnical Journal 27 (4), 409–417. https://doi.org/10.1139/t90-057.

Bollati, I.M., Cavalli, M., 2021. Unraveling the relationship between geomorphodiversity and sediment connectivity in a small alpine catchment. Transactions in GIS 25, 2481–2500. https://doi.org/10.1111/tgis.12793.

Bonn, A., Allott, T., Hubacek, K., Stewart, J., 2009. Introduction – drivers of change in upland environments: concepts, threats and opportunities. In: Bonn, A., Allott, T., Hubacek, K., Stewart, J. (Eds.), Drivers of Environmental Change in Uplands. Routledge, Abingdon, Oxfordshire, pp. 1–10.

Borselli, L., Cassi, P., Torri, D., 2008. Prolegomena to sediment and flow connectivity in the landscape: a GIS and field numerical assessment. Catena 75 (3), 268–277. https://doi.org/10.1016/j.catena.2008.07.006.

Brayshaw, D., Hassan, M.A., 2009. Debris flow initiation and sediment recharge in gullies. Geomorphology 109 (3–4), 122–131. https://doi.org/10.1016/j.geomorph.2009.02.021.

British Geological Survey, 1987. Moffat, Scotland Sheet 16W, Drift. 1:50 000 Geology Series. British Geological Survey, Keyworth, Nottingham.

British Geological Survey, 2009. Moffat, Scotland Sheet 16W, Bedrock. 1:50 000 Geology Series. British Geological Survey, Keyworth, Nottingham.

Burbank, D.W., Leland, J., Fielding, E., Anderson, R.S., Brosovic, N., Reid, M., Duncan, C., 1996. Bedrock incisions, rock uplift and threshold hillslopes in the northwestern Himalayas. Nature 379, 505–510. https://doi.org/10.1038/379505a0.

Burian, L., Šujan, M., Stankoviansky, M., Šilhavy, J., Okai, A., 2017. Dependence of gully networks on faults and lineament networks, case study from Hronska, Pahorkatina Hill Land. Open Geoscience 9, 101–113. https://doi.org/10.1515/geo-2017-0008.

Carter, G.D.O., Cooper, R., Gafeira, J., Howe, J.A., Long, D., 2020. Morphology of small-scale submarine mass movement events across the northwest United Kingdom. Geomorphology 365, 107282. https://doi.org/10.1016/j.geomorph.2020.107282.

Cavalli, M., Trevisani, S., Comiti, F., Marchi, L., 2013. Geomorphometric assessment of spatial sediment connectivity in small Alpine catchments. Geomorphology 188, 31–41. https://doi.org/10.1016/j.geomorph.2012.05.007.

Choi, J.-H., Edwards, P., Ko, K., Kin, Y.-S., 2016. Definition and classification of fault damage zones: a review and a new methodological approach. Earth-Science Reviews 152, 70–87. https://doi.org/10.1016/j.earscirev.2015.11.006.

Cogné, N., Doepke, D., Chew, D., Stuart, F.M., Mark, C., 2016. Measuring plume-related exhumation of the British Isles in Early Cenozoic times. Earth and Planetary Science Letters 456, 1–15. https://doi.org/10.1016/j.epsl.2016.09.053.

DiBiase, R.A., Rossi, M.W., Neely, A.B., 2018. Fracture density and grain size controls on the relief structure of bedrock landscapes. Geology 46 (5), 399–402. https://doi.org/10.1130/G40006.1.

Fame, M.L., Spotila, J.A., Owen, L.A., Dortch, J.M., Shuster, D.L., 2018. Spatially heterogeneous post-Caledonian burial and exhumation across the Scottish Highlands. Lithosphere 10 (3), 406–425. https://doi.org/10.1130/L678.1.

Faulkner, D.R., Jackson, C.A.L., Lunn, R.J., Schlische, R.W., Shipton, Z.K., Wibberley, C.A.J., Withjack, M.O., 2010. A review of recent developments concerning the structure, mechanics and fluid flow properties of fault zones. Journal of Structural Geology 32, 1557–1575. https://doi.org/10.1016/j.jsg.2010.06.009.

Finlayson, A., 2020. Glacial conditioning and paraglacial sediment reworking in Glen Croe (the Rest and Be Thankful), western Scotland. Proceedings of the Geologists' Association 131 (2), 138–154. https://doi.org/10.1016/j.pgeola.2020.02.007.

Firth, C.R., Stewart, I.S., 2000. Postglacial tectonics of the Scottish glacio-isostatic uplift centre. Quaternary Science Reviews 19 (14–15), 1469–1493. https://doi.org/10.1016/S0277-3791(00)00074-3.

Fryirs, K., 2013. (Dis)connectivity in catchment sediment cascades: a fresh look at the sediment delivery problem. Earth Surface Processes and Landforms 38, 30–46. https://doi.org/10.1002/esp.3242.

Fryirs, K.A., Brierley, G.J., Preston, N.J., Kasai, M., 2007. Buffers, barriers and blankets: the (dis)connectivity of catchment-scale sediment cascades. Catena 70 (1), 49–67. https://doi.org/10.1016/j.catena.2006.07.007 (ISSN 0341-8162).

Gordon, J.E., Stone, P., 2021. Scotland: geological foundations and landscape evolution. In: Ballantyne, C.K., Gordon, J.E. (Eds.), Landscapes and Landforms of Scotland, World Geomorphological Landscapes. Springer, Cham https://doi.org/10.1007/978-3-030-71246-4_2.

Haeberli, W., Schaub, Y., Huggel, C., 2017. Increasing risks related to landslides from degrading permafrost into new lakes in deglaciating mountain ranges. Geomorphology 293 (Part B), 405–417. https://doi.org/10.1016/j.geomorph.2016.02.009.

Hall, A.M., Gillespie, M.R., 2017. Fracture controls on valley persistence: the Cairngorm Granite pluton, Scotland. International Journal of Earth Sciences 106, 2203–2219. https://doi.org/10.1007/s00531-016-1423-z.

Harvey, A.M., 1991. The influence of sediment supply on the channel morphology of upland streams: Howgill Fells, northwest England. Earth Surface Processes and Landforms 16, 675–684. https://doi.org/10.1002/esp.3290160711.

Hoek, E., 1999. Putting numbers to geology – and engineer's viewpoint. Quarterly Journal of Engineering Geology 32, 1–19.

Hoek, E., Brown, E.T., 2019. The Hoek–Brown failure criterion and GSI — 2018 edition. Journal of Rock Mechanics and Geotechnical Engineering 11 (3), 445–463. https://doi.org/10.1016/j.jrmge.2018.08.001.

Holford, S.P., Green, P.F., Hillis, R.R., Underhill, J.R., Stoker, M.S., Duddy, I.R., 2010. Multiple post-Caledonian exhumation episodes across NW Scotland revealed by apatite fission-track analysis. Journal of the Geological Society, London 167, 675–694. https://doi.org/10.1144/0016-76492009-167.

Hudson, J.D., 2011. Discuss on 'Multiple post-Caledonian exhumation episodes across NW Scotland revealed by apatite fission-track analysis'. Journal of the Geological Society of London 168 (2011), 1225–1226. https://doi.org/10.1144/0016-76492011-030.

Hungr, O., Leroueil, S., Picarelli, L., 2013. The Varnes classification of landslide types, an update. Landslides 11, 167–194. https://doi.org/10.1007/s10346-013-0436-y.

Jarman, D., Harrison, H., 2019. Rock slope failure in the British Mountains. Geomorphology 340, 202–233. https://doi.org/10.1016/j.geomorph.2019.03.002.

Kirkby, M.J., Bracken, L.J., 2009. Gully processes and gully dynamics. Earth Surface Processes and Landforms 34, 1841–1851. https://doi.org/10.1002/esp.1866.

Kondolf, G.M., Gao, Y., Annandale, G.W., Morris, G.L., Jiang, E., Zhang, J., Cao, Y., Carling, P., Fu, K., Gou, Q., Hotchkiss, R., Peteuil, C., Sumi, T., Wang, H., Wang, Z., Wei, Z., Wu, B., Wu, C., Wang, C.T., 2014. Sustainable sediment management in reservoirs and regulated rivers: experiences from five continents. Earth's Future 2 (5), 256–280. https://doi.org/10.1002/2013EF000184.

Kovac, M., Synak, R., Fordinal, K., Joniak, P., Toth, C., Vojtko, R., Nagy, A., Barath, I., Maglay, J., Minar, J., 2011. Late Miocene and Pliocene history of the Danube Basin: inferred from development of depositional systems and timing of sedimentary facies changes. Geologica Carpathica 62 (6), 519–534. https://doi.org/10.2478/v10096-011-0037-4 (1335-0552).

Kumar, P.S., Head, J.W., Kring, D.A., 2010. Erosional modification and gully formation at Meteor Crater, Arizona: insights into crater degradation processes on Mars. Icarus 208, 608–620. https://doi.org/10.1016/j.icarus.2010.03.032.

Loye, A., Pedrazzini, A., Theule, J.I., Jaboyedoff, M., Liébault, F., Metzger, R., 2012. Influence of bedrock structures on the spatial pattern of erosional landforms in small alpine catchments. Earth Surface Processes and Landforms 37, 1407–1423. https://doi.org/10.1002/esp.3285.

Łuszczak, K., Persano, C., Stuart, F., 2014. Low temperature thermochronological constraints on the Cenozoic evolution of the Lake District and Southern Uplands Massifs (NW England, SW Scotland). 14th International Conference on Thermochronology (Chamonix, France).

Manjoro, M., 2015. Structural control of fluvial drainage in the western domain of the Cape Fold Belt, South Africa. Journal of African Earth Sciences 101, 350–359. https://doi.org/10.1016/j.jafrearsci.2014.10.001.

May, C.L., Gresswell, R.E., 2004. Spatial and temporal patterns of debris-flow deposition in the Oregon Coast Range, USA. Geomorphology 57, 135–149. https://doi.org/10.1016/S0169-555X(03)00086-2.

Messenzehl, K., Hoffmann, T., Dikau, R., 2014. Sediment connectivity in the high-alpine valley of Val Müschauns, Swiss National Park — linking geomorphic field mapping with geomorphometric modelling. Geomorphology 221, 215–229. https://doi.org/10.1016/j.geomorph.2014.05.033.

Mitchell, T.M., Faulkner, D.R., 2012. Towards quantifying the matrix permeability of fault damage zones in low porosity rocks. Earth and Planetary Science Letters 339-340, 24–31.

Molnar, P., Anderson, R.S., Anderson, S.P., 2007. Tectonics, fracturing of rock, and erosion. Journal of Geophysical Research 112, F3014. https://doi.org/10.1029/2005JF000433.

Neely, A.B., DiBiase, R.A., 2020. Drainage area, bedrock fracture spacing, and weathering controls on landscape-scale patterns in surface sediment grain size. Journal of Geophysical Research - Earth Surface 125, e2020JF005560. https://doi.org/10.1029/2020JF005560.

Neely, A.B., DiBiase, R.A., Corbett, L.B., Bierman, P.R., Caffee, M.W., 2019. Bedrock fracture density controls on hillslope erodibility in steep rocky landscapes with patchy soil cover, southern California, USA. Earth and Planatary Science Letters 522 (15), 186–197. https://doi.org/10.1016/j.epsl.2019.06.011.

Norbury, D., 2021. Ground models; a brief overview. Quarterly Journal of Engineering Geology and Hydrogeology 54, 2. https://doi.org/10.1144/qjegh2020-018.

Novitski, C.G., Holbrook, S.W., Carr, B.J., Pasquet, S., Okaya, D., Flinchum, B.A., 2018. Mapping inherited fractures in the critical zone using seismic anisotropy from circular surveys. Geophysical Research Letters 45 (7), 3126–3135. https://doi.org/10.1002/2017GL075976.

Owen, R., Maziti, A., Dahlin, T., 2007. The relationship between regional stress field, fracture orientation and depth of weathering and implications for groundwater prospecting in crystalline rocks. Hydrogeology Journal 15, 1231–1238. https://doi.org/10.1007/s10040-007-0224-7.

Palamakumbura, R., Krabbendam, M., Whitbread, K., Arnhardt, C., 2020. Data acquisition by digitizing 2-D fracture networks and topographic lineaments in geographic

information systems: further development and applications. Solid Earth 11, 1731–1746. https://doi.org/10.5194/se-11-1731-2020.
Palamakumbura, R., Finlayson, A., Ciurean, R., Nedumpallile-Vasu, N., Freeborough, K., Dashwood, C., 2021. Geological and geomorphological influences on a recent debris flow event in the ice-scoured mountain Quaternary domain, western Scotland. Proceedings of the Geologists' Association 132 (4), 456–468. https://doi.org/10.1016/j.pgeola.2021.05.002.
Pearce, D., Rea, B.R., Bradwell, T., McDougall, D., 2014. Glacial geomorphology of the Tweedsmuir Hills, Central Southern Uplands, Scotland. Journal of Maps 10 (3), 457–465. https://doi.org/10.1080/17445647.2014.886492.
Ragg, J.M., Bibby, J.S., 1966. Frost weathering and solifluction products in Southern Scotland. Geofiska Annaler, Series A, Physical Geography 48, 12–23. https://doi.org/10.1080/04353676.1966.11879724.
Reid, M.E., LaHusen, R.G., Iverson, R.M., 1997. Debris-flow initiation experiments using diverse hydrologic triggers. Proceedings of the 1997 1st International Conference on Debris Flow Hazards Mitigation: Mechanics, Prediction and Assessment, p. 11.
Roy, S.G., Tucker, G.E., Koons, P.O., Smith, S.M., Upton, P., 2016. A fault runs through it: modeling the influence of rock strength and grain-size distribution in a fault-damaged landscape. Journal of Geophysical Research, Earth Surface 121, 1911–1930. https://doi.org/10.1002/2015JF003662.
Scott, D.N., Wohl, E.E., 2018. Bedrock fracture influences on geomorphic process and form across process domains and scales. Earth Surface Processes and Landforms 44, 27–45. https://doi.org/10.1002/esp.4473.
Shobe, C.M., Tucker, G.E., Anderson, R.S., 2016. Hillslope-derived blocks retard river incision. Geophysical Research Letters 43, 5070–5078. https://doi.org/10.1002/2016GL069262.
Singhal, B.B.S., Gupta, R.P., 2010. Applied Hydrogeology of Fractured Rocks. Springer Science and Business Media, Berlin.
Sklar, L.S., Riebe, C.S., Marshall, J.A., Genetti, J., Leclere, S., Lukens, C.L., Merces, V., 2017. The problem of predicting the size distribution of sediment supplied by hillslopes to rivers. Geomorphology 277, 31–49. https://doi.org/10.1016/j.geomorph.2016.05.005.
Sklar, L.S., Riebe, C.S., Genetti, J., Leclere, S., Lukens, C.L., 2020. Downvalley fining of hillslope sediment in an alpine catchment: implications for downstream fining of sediment flux in mountain rivers. Earth Surface Processes and Landforms 45, 1828–1845. https://doi.org/10.1002/esp.4849.
Stone, P., 2014. The Southern Uplands Terrane in Scotland – a notional controversy revisited. Scottish Journal of Geology 50 (2), 97–123. https://doi.org/10.1144/sjg2014-001.
Stone, P., McMillan, A.A., Floyd, J.D., Barnes, R.P., Phillips, E.R., 2012. British Regional Geology: South of Scotland. Fourth edition. British Geological Survey, Keyworth, Nottingham.
Sugden, D.E., 1968. The selectivity of glacial erosion in the Cairngorm Mountains, Scotland. Transactions of the Institute of British Geographers 45, 79–92. https://doi.org/10.2307/621394.
Thomas, C.W., Gillespie, M.R., 2004. Geological Structure and Landscape of the Cairngorm Mountains, Comissioned report, Scottish Natural Heritage 121pp.
Twidale, C.R., 2004. River patterns and their meaning. Earth-Science Reviews 67 (3–4), 159–218. https://doi.org/10.1016/j.earscirev.2004.03.001.
Wang, X., Frattini, P., Stead, D., Sun, J., Liu, H., Valagussa, A., Li, L., 2020. Dynamic rockfall risk analysis. Engineering Geology 272, 105622. https://doi.org/10.1016/j.enggeo.2020.105622 (ISSN 0013-7952).
Wang, X., Crosta, G.B., Clague, J.J., Stead, D., Sun, J., Qi, S., Liu, H., 2021. Fault controls on spatial variation of fracture density and rock mass strength within the Yarlung Tsangpo Fault damage zone (southeastern Tibet). Engineering Geology 291, 106238 ISSN 0013-7952, https://doi.org/10.1016/j.enggeo.2021.106238.
Willgoose, G., Bras, R.L., Rodriguez-Iturbe, I., 1991. A coupled channel network growth and hillslope evolution model: 1. Theory, Water Resources Research 27 (7), 1671–1684. https://doi.org/10.1029/91WR00935.
Winter, M.G., Shearer, B., Palmer, D., Peeling, D., Harmer, C., Sharpe, J., 2016. The economic impact of landslides and floods on the road network. Procedia Engineering 143, 1425–1434. https://doi.org/10.1016/j.proeng.2016.06.168.
Wolf, S.G., Huismans, R.S., Braun, J., Yuan, X., 2022. Topography of mountain belts controlled by rheology and surface processes. Nature 606, 516–521. https://doi.org/10.1038/s41586-022-04700-6.
Woodcock, N., Strachan, R., 2012. The Geological History of Britain and Ireland. 2nd edition. Wiley-Blackwell, Oxford.